NACA RM L52L01a

NACA

RESEARCH MEMORANDUM

THE INFLUENCE OF VORTEX GENERATORS ON THE PERFORMANCE OF A SHORT 1.9:1 STRAIGHT-WALL ANNULAR DIFFUSER WITH A WHIRLING INLET FLOW

By Charles C. Wood and James T. Higginbotham

Langley Aeronautical Laboratory
Langley Field, Va.

NATIONAL ADVISORY COMMITTEE
FOR AERONAUTICS

WASHINGTON

February 9, 1953

41

NATIONAL ADVISORY COMMITTEE FOR AERONAUTICS

RESEARCH MEMORANDUM

THE INFLUENCE OF VORTEX GENERATORS ON THE PERFORMANCE OF A SHORT 1.9:1 STRAIGHT-WALL ANNULAR DIFFUSER WITH A WHIRLING INLET FLOW

By Charles C. Wood and James T. Higginbotham

SUMMARY

An investigation was conducted in a duct system having fully developed pipe flow to determine the effects of vortex generators on the performance of a diffuser having a whirling inlet flow. The annular diffuser had a constant 21-inch outer diameter, an over-all equivalent conical expansion angle of 15°, and a 1.9:1 area ratio. Tests of the diffuser having mean inlet whirl angles of 0°, 15.2°, and 20.6° were made. The vortex generators used in this investigation were rectangular, noncambered airfoils, which were varied in chord, span, angle setting, number, and location.

Without vortex generators, the diffuser separated approximately 5 inches downstream of the cylinder-cone junction except for the 20.6° inlet whirl angle for which no separation was observed. An arrangement consisting of vortex generators on both the diffuser inner and outer walls and representing the best compromise arrangement for all inlet whirl angles tested eliminated separation and resulted in improvements in static-pressure coefficient above that noted for no control of 11, 20, and 23 percent, respectively, for the 0°, 15.2°, and 20.6° whirl angles.

INTRODUCTION

Research to determine an efficient combination of turbojet and afterburner indicates that improvements in the diffusion of gases from the turbine to the afterburner are necessary to realize more fully the potential of the power plant. The internal geometry of the system and space limitations lead to consideration of the short annular diffuser, of which the annular diffuser of constant outer-wall diameter is typical.

Some data on the performance of annular diffusers of constant outer-wall diameter are available. Tests of an annular diffuser with vortex

generators having an axial inflow and a thick inlet boundary layer are reported in reference 1. Other tests of annular diffusers having 0° and finite inlet whirl angles are reported, respectively, in references 2 and 3.

Reference 1 indicates that flow separation from the inner wall of the diffuser tested seriously impaired the performance from the standpoint of static-pressure increase, total-pressure loss, and stability of operation. It has also been shown in reference 1 that the seriousness of these problems can be greatly reduced for axial inlet flow by delaying or eliminating separation and that this effect can be accomplished by the vortex-generator principle. It is of immediate interest to determine the influence of a whirling inlet flow, which is known to exist behind conventional turbines, on the performance of a diffuser with various vortex-generator arrangements. In the search for efficient control at all inlet whirl angles, two methods of control, that of the vortex-generator principle and that of conversion of rotational energy to static pressure by straightening the flow, are investigated and reported herein.

The investigation was made by using an available representative annular diffuser having a constant outer-wall diameter. NACA 0012 airfoils, which were used as straightening vanes and as vortex generators, were varied in chord, span, spacing, angle setting, and location. The investigation was conducted with fully developed pipe flow and with angles of whirl up to approximately 21° at the diffuser inlet. The mean inlet Mach number was varied from approximately 0.15 to 0.40, the resulting maximum Reynolds number being approximately 1.28×10^6 when based on the inlet hydraulic diameter.

SYMBOLS

p	static pressure
H	total pressure
χ	whirl angle measured with respect to diffuser center line, deg
ρ	density
μ	coefficient of viscosity
u	local velocity
U	maximum velocity across an annular section
y	perpendicular distance from either the diffuser inner or outer walls, in.

r radius of duct, in.

$\bar{p}$ weighted static pressure, $\dfrac{\int_{r_1}^{r_2} \rho u p r dr}{\int_{r_1}^{r_2} \rho u r dr}$

$\bar{H}$ weighted total pressure, $\dfrac{\int_{r_1}^{r_2} \rho u H r dr}{\int_{r_1}^{r_2} \rho u r dr}$

$\bar{q}_c$ impact pressure, $\bar{H} - \bar{p}$

$\bar{\chi}$ weighted whirl angle, $\dfrac{\int_{r_1}^{r_2} \rho u \chi r dr}{\int_{r_1}^{r_2} \rho u r dr}$, deg

D_i hydraulic diameter, 0.541 or $\dfrac{4 \text{ cross-sectional area of duct}}{\text{Perimeter of duct}}$

R_i Reynolds number, $\dfrac{p_i V_i D_i}{\mu i}$

$\dfrac{\overline{\Delta p}}{\bar{q}_{ci}}$ static-pressure coefficient, $\dfrac{\bar{p}_e - \bar{p}_i}{\bar{q}_{ci}}$

$\dfrac{\overline{\Delta H}}{\bar{q}_{ci}}$ diffuser loss coefficient, $\dfrac{\bar{H}_i - \bar{H}_e}{\bar{q}_{ci}}$

δ boundary-layer thickness

δ^* boundary-layer displacement thickness, $\int_0^{\delta} \left(1 - \frac{u}{U}\right) dy$

θ boundary-layer momentum thickness, $\int_0^{\delta} \frac{u}{U}\left(1 - \frac{u}{U}\right) dy$

$\frac{\delta^*}{\theta}$ boundary-layer shape parameter

Subscripts:

i diffuser inlet station

e diffuser exit station

a axial component

1 reference to diffuser inner wall

2 reference to diffuser outer wall

APPARATUS AND PROCEDURE

Test equipment.- A schematic drawing of the experimental setup is shown in figure 1. A more detailed drawing of the immediate area of the diffuser is shown in figure 2.

The setup consisted of an annular diffuser of constant outer diameter preceded by a section of annular ducting approximately 27 feet long. The diffuser had an outer diameter of 21 inches, an area ratio of 1.9 to 1, and an over-all equivalent conical angle of expansion of 15°. The upstream annular ducting had a constant inner diameter of $14\frac{1}{2}$ inches and an outer diameter varying between 21 and 25 inches. The juncture between the inner cylinder and the cone of the diffuser was faired to a 16-inch radius. Air entered the test apparatus through a cylindrical settling screen which was covered with open-mesh cloth. From this chamber air flowed through an inlet bell, through the stator, and through 27 feet of annular ducting to the diffuser inlet. The quantity of air passing through the experimental setup was controlled by a variable-speed exhauster connected far downstream of the diffuser exit.

Instrumentation.- Stream total pressures, static pressures, and whirl angles were measured by remote-controlled survey instruments at

the diffuser inlet and diffuser exit stations (fig. 2). A drawing of the survey instrument is shown in figure 3. Flow surveys were made at only one station at a time so that there were no instruments in the stream ahead of the measuring station. These surveys were made at four circumferential positions at each of the survey stations. Results are based upon the average of all four circumferential positions.

Static orifices extending from upstream of the diffuser inlet station to a point 21 inches downstream of the exit station were installed along a single generatrix on the outer wall. Static orifices extending from approximately the diffuser inlet station to a point 7 inches upstream of the diffuser exit station were located along three equally spaced generatrices on the inner wall of the diffuser.

Small tufts which were found to have no influencing effects on diffuser performance were used to observe the flow in the diffuser. These tufts were fastened along four generatrices approximately 90° apart on both inner and outer walls of the diffuser and were viewed through transparent windows in the outer wall of the diffuser.

Vortex generators.- The size and arrangement of the vortex generators were varied. All vortex generators were NACA 0012 airfoil sections with chords of 1 to 3 inches and spans of $\frac{1}{2}$ to $3\frac{1}{8}$ inches. The number of vortex generators varied from 12 to 48 units; however, most of the tests utilized 24 units.

The angle setting of a vortex generator refers to the angle between the center line of the vortex generator and the diffuser center line. When the angle between the diffuser center line and the vortex-generator center line lies in the same quadrant as the angle between the diffuser center line and the direction of flow, the angle setting is referred to as positive; when the angles lie in different quadrants, the angle setting is referred to as negative. The longitudinal position of the vortex generators is referenced to a plane passing through the 30-percent-chord station. Vortex generators attached to the inner wall in most cases were located about 1 inch upstream of the cylinder-cone junction. This location is approximately 5 inches upstream of the line of separation of this diffuser when having an axial inlet flow. Tests were conducted with vortex generators located simultaneously at the above station and at another station immediately downstream. Tests were also conducted with vortex generators located on the outer wall 2 inches upstream of the cylinder-cone junction. Unless otherwise specified, however, the vortex generators were mounted on the inner wall 1 inch upstream of the cylinder-cone junction. A complete list of all vortex-generator arrangements tested is given in table I.

Basis of comparison of the effectiveness of vortex generators.- The fluctuating flow often observed at the exit of wide-angle diffusers was not observed in this investigation. Within the limits of frequency response of the measuring instrument the flow can be considered stable; therefore, measurements were made at the diffuser exit rather than in the tail pipe.

The effectiveness of each vortex-generator configuration on the performance of the annular diffuser has been compared on the basis of the static-pressure coefficient $\overline{\Delta p}/\overline{q}_{ci}$, of loss coefficient $\overline{\Delta H}/\overline{q}_{ci}$, and whirl angle $\overline{\chi}$. Longitudinal distribution of static pressure $\frac{p - \overline{p}_i}{\overline{q}_{ci}}$, and radial distributions of static pressure $\frac{p - \overline{p}_i}{\overline{q}_{ci}}$, total pressure $\frac{\overline{H}_i - H}{\overline{q}_{ci}}$, and flow angle χ are presented for some configurations.

THEORY

The principle by which the vortex generator acts to achieve more efficient diffusion is generally known and constitutes control of flow separation by a process of reenergizing the low-energy regions of the boundary layer with higher energy air.

One of the basic principles of an ideal fluid possessing a whirling motion is the preservation of angular momentum. In order to maintain constant angular momentum through a diffuser of the type tested, an increase in the angle of flow is required and the unrecoverable tangential component of kinetic energy is increased; thus, a restriction on the rise in static pressure is established. The whirling motion is responsible for other unfavorable as well as favorable flow characteristics. For instance, a radial pressure gradient which assists divergence of the flow is established by a centrifugal force, which acts upon the air to create higher static pressures near the diffuser outer wall; a centripetal flow of low-energy air which is conductive to boundary-layer separation at low flow angles and retards separation at large whirl angle is also established. This phenomenon has been discussed in detail in reference 3.

Increases in the static-pressure coefficient can be realized by conversion of the energy of rotation in the diffuser to static-pressure energy by efficient straightening of the flow. As an example, diffusion of an ideal fluid with an inlet whirl angle of 20.6° in a 1.9:1 area ratio diffuser would realize a static-pressure coefficient of 0.67. A

pressure coefficient of 0.76 would be realized by conversion of all the kinetic energy in the diffuser.

RESULTS AND DISCUSSION

Before the performance of a diffuser can be evaluated, the nature of the flow entering the diffuser must be known. Accordingly, pressure surveys were made at four equally spaced circumferential stations at the diffuser inlet for flows having inlet whirl angles of 0°, 15.2°, and 20.6°, at Mach numbers from approximately 0.15 to 0.4. Average total pressures, static pressures, and inlet whirl angles from the four rakes are presented in figure 4 for an inlet pressure ratio of approximately 0.95. The inlet velocity profiles and the associated boundary-layer properties observed for 0° inlet whirl angle are presented in figure 5.

20.6° Inlet Whirl Angle

The loss coefficient $\overline{\Delta H}/\overline{q}_{ci}$, static-pressure coefficient $\overline{\Delta p}/\overline{q}_{ci}$, exit whirl angle $\overline{\chi}_e$, longitudinal static pressures, and radial distributions of total pressure, static pressure, and exit whirl angle are presented in figures 6 to 16 for the diffuser with and without vortex generators. The two coefficients, in most cases, are presented as a function of the axial inlet pressure ratio $\overline{p}_i/\overline{H}_{ia}$.

The flow along both walls for the diffuser without vortex generators, as indicated by tufts, was attached. The angle of whirl was observed to increase through the diffuser, as expected. The small span counter-rotating and corotating vortex-generator arrangements, in general, reduced or eliminated the whirling motion near the inner wall. The largest span arrangement located on the inner wall resulted in approximately axial flow on the outer wall with separation on the inner wall; this condition was not observed with generators of other spans nor was it observed with the same generator on the outer wall.

A maximum static-pressure coefficient and minimum loss coefficient of 0.49 and 0.07, respectively, were observed for the diffuser without vortex generators (fig. 6). The whirl angle increased through the diffuser from a mean inlet whirl angle of 20.6° to a mean exit whirl angle of 43°.

The optimum vortex-generator arrangement tested for the diffuser of reference 1 $\left(24\ 3\text{-inch-chord}, \frac{1}{2}\text{-inch-span generators, counterrotating, angle setting } \pm 15^\circ\right)$ has been tested and the results are presented in

figure 7. Also presented are results for the same arrangement at different angle settings, and for an arrangement consisting of small-span generators near the inlet with large-span generators 9 inches downstream. (See arrangement 4, table I.) The arrangements with small span results in no increase in pressure coefficient, except at low speeds, and in increases in loss coefficient. Arrangement 4 results in 5-percent increase in pressure coefficient, 13-percent increase in loss coefficient, and 19-percent reduction in exit whirl angle. All other tests, except when using separate vortex generators simultaneously for straightening the flow and for controlling separation, were conducted with the vortex generators set for corotation. The vortex-generator chord, span, number of generators, and angle setting were varied, respectively, from 1 to 3 inches, $\frac{1}{2}$ to $3\frac{1}{8}$ inches, 12 to 48, and 6° to -15°. The location was also varied.

Vortex-generator span.- Increasing the vortex-generator span (fig. 8) increases the pressure and loss coefficients and decreases the exit whirl angle. The $1\frac{9}{16}$-inch-span generator arrangement is possibly the better because the pressure coefficient almost equals that of the $3\frac{1}{8}$-inch-span generator arrangement and the loss coefficient is much less.

The increase in the pressure coefficient with increasing span can be associated with greater conversion of the kinetic energy of rotation to static pressure, as would be expected by theory. The increase in loss coefficient with increase in span is not surprising since the vortex generators are at large angles of attack.

Vortex-generator angle setting and span.- The effect of vortex-generator angle setting on the static-pressure coefficient, loss coefficient, and whirl angle for several vortex-generator spans are presented in figure 9. The highest static-pressure coefficient (0.55) was observed with the $3\frac{1}{8}$-inch-span generator at 0° angle setting. This value represents an increase of 18 percent over that for the diffuser with no generators; however, this increase occurs at the expense of an increase in loss coefficient of approximately 100 percent. The corresponding whirl angle has been reduced from 43° to 3.5°.

The orientation and trend of the curves on this figure, except the loss-coefficient curve for the arrangement with $3\frac{1}{8}$-inch-span generators, are, in general, as would have been expected.

The effect of span and angle setting of the vortex generators on the radial distribution of exit total and static pressure and whirl

angle are of considerable interest and are presented in figure 10. Also included on this figure are the inlet data, exit data for the diffuser without vortex generators, and exit data for the diffuser with counter-rotating vortex-generator arrangements. The favorable distribution of total and static pressure and whirl angle observed near the outer wall as well as the unfavorable distribution observed near the inner wall for the diffuser without vortex generators are theoretically predictable and have been previously shown in the experimental investigation of reference 3. In general, it appears that the total-pressure distribution near the inner wall, as well as across the entire diffuser, is more favorable when the vortex-generator arrangement has an angle setting which gives whirl angles near 0° on the inner wall. This condition is true also for the static pressure.

The longitudinal static pressures on both the diffuser inner and outer walls for the diffuser with and without vortex generators are shown in figure 11. On the inner wall the static pressures at the diffuser exit were obtained from the static tube on one of the survey probes. Immediately downstream of the diffuser inlet on the diffuser inner wall, a local acceleration (indicated by a decrease in static pressure) of flow was noted and can be attributed to sharp curvature of the inner wall. The static pressure on the inner wall for the diffuser without generators and with the counterrotating arrangements reaches a maximum approximately 14 inches downstream of the inlet station, but decreases rapidly from this location to the diffuser exit. This decrease results from loss of total pressure along the inner wall by centripetal flow of low-energy air and increased whirl motion as expected. The conversion of energy is practically complete at the exit station, as has been previously shown in reference 3.

Vortex-generator chord.- The effect of vortex-generator chord on the static-pressure coefficient, loss coefficient, and exit whirl angle is shown in figure 12 as a function of inlet pressure ratio and the radial distribution of total pressure, static pressure, and whirl angle is shown in figure 13. These tests indicate no significant effect on the mean total and static pressures. Increasing vortex-generator chord results progressively in reductions in the radial variations of total and static pressures. The 2- and 3-inch-chord generators overturn the flow near the diffuser center and result in larger radial variation of whirl angle than noted for the 1-inch-chord arrangement and for no control.

Vortex-generator number.- The performance coefficients and exit whirl angle, shown in figure 14, and the exit radial distribution of total pressure, static pressure, and whirl angle, shown in figure 15, indicate the arrangement with 12 generators to be the most efficient. This arrangement has the lowest loss coefficient, as expected, maximum pressure coefficient, and less radial variation of the exit total pressure, static pressure, and whirl angle.

A multiple vortex-generator arrangement.- A single arrangement (arrangement 23, table I) with large-span generators for conversion of all rotational energy and small-span generators for controlling separation, both conditions being necessary for maximum pressure coefficient, was tested. Separation from the inner wall was observed; thus practically no change in the loss coefficient and pressure coefficient from that observed for the large-span arrangement by itself occurred. The failure to eliminate or delay separation was possibly because the small generators were located near the point of separation. Model difficulties prevented continuation of this particular phase of the investigation.

Vortex generators on the outer wall.- Two arrangements with vortex generators on the outer wall were tested (arrangements 24 and 25, table I). A photograph of the model with arrangement 25, taken through the transparent sections of the side wall, is shown in figure 17. No separation was observed for either arrangement. The pressure coefficient, loss coefficient, and exit whirl angle presented in figure 16 indicate the respective coefficients for the two arrangements to be essentially the same with arrangement 25 representing 23-percent increase and 5-percent decrease when compared with the respective coefficients observed for the diffuser without vortex generators. These two arrangements combine the favorable effects of eliminating flow separation and the conversion of rotational energy and have therefore proven to be the most efficient arrangements tested.

The significant improvement in performance of the large-span arrangement located on the outer wall (arrangement 24) when compared with the same arrangement located on the inner wall (arrangement 17) is attributed to the establishment by arrangement 24 of tip vortices near the inner wall rather than near the outer wall and the consequent elimination of separation.

15.2° Inlet Whirl Angle

The loss coefficient, static-pressure coefficient, and exit whirl angle for all of the configurations tested are presented as a function of inlet pressure ratio in figure 18. The vortex-generator arrangements tested are presented in table I.

The diffuser without vortex generators was observed to separate on the inner wall approximately 5 inches downstream of the cylinder-cone junction. The small-span vortex-generator arrangements on the inner wall eliminated separation as did all arrangements on the outer wall. The flow along the outer wall was attached and whirling at large angles except when the generator arrangements were located on the outer wall, in which case the flow was approximately axial.

A maximum static-pressure coefficient and a minimum loss coefficient of 0.51 and 0.11, respectively, were observed for the diffuser without vortex generators (fig. 18). Vortex-generator arrangement 25 consisting of generators on both walls is unquestionably the most efficient arrangement tested from the standpoint of the pressure and loss coefficients. This arrangement results in an 18-percent increase in pressure coefficient with a 27-percent decrease in loss coefficient when compared with the diffuser without generators. Arrangement 24 also resulted in a substantial improvement; however, two of the arrangements with $\frac{1}{2}$-inch span (arrangements 1 and 8) and the multiple arrangement (arrangement 4) were approximately as effective. The arrangements with large-span generators on the inner wall were of no benefit to the pressure coefficient and a serious handicap to loss coefficient. Examination of the curves for the various vortex-generator arrangements discussed previously indicate greater improvement of pressure coefficient is realized by eliminating flow separation from the inner wall than by conversion of the tangential kinetic energy. This condition is not necessarily true for all inlet whirl angles.

0° Inlet Whirl Angle

The loss coefficient, static-pressure coefficient, and the exit whirl angle are presented as a function of inlet pressure ratio in figure 19 for the diffuser without generators and with all generator arrangements tested.

The diffuser without vortex generators was observed to separate on the inner wall approximately 5 inches downstream of the cylinder-cone junction. Each vortex-generator arrangement tested eliminated flow separation; however, two arrangements (arrangements 2 and 8, table I) established a large whirling motion near the inner wall. Flow on the outer wall was axial, as expected.

A maximum static-pressure coefficient and a minimum loss coefficient of 0.52 and 0.10, respectively, were observed for the diffuser without vortex generators. All arrangements tested increased the pressure coefficient above that for no control; however, vortex generator arrangement 1, the optimum arrangement for 0° inflow (ref. 1), is unquestionably the best configuration tested. The arrangement with vortex generators on both walls, an arrangement obviously not designed for 0° axial flow, indicates a decrease in pressure coefficient and an increase in loss coefficient when compared with the respective coefficients of arrangement 1. The difference in coefficient for the two arrangements results from loss attributed to skin friction of the large generators.

Effect of Inlet Whirl Angle on Diffuser Performance

The influence of the inflow (inlet whirl) angle on the static-pressure coefficient, total-pressure coefficient, and exit whirl angle of an annular diffuser with several different vortex-generator arrangements is presented in figure 20; the influence of inflow angle on the radial distribution of the total pressure, static pressure, and whirl angle at the diffuser exit is presented in figure 21. The longitudinal static-pressure distributions for the arrangement with generators on both walls are presented in figure 22.

Diffuser performance.- The curve for the diffuser without generators (fig. 20) indicates decreasing pressure coefficients with increasing inflow angles. Insufficient data are available for determining whether this is a regular decrease or whether irregularities might exist at intermediate inflow angles. The angle of inflow does obviously influence the effectiveness of some vortex-generator arrangements from the standpoint of pressure and loss coefficients. As an example, arrangement 1 realized 15-, 10-, and 2-percent increase in the static-pressure coefficient, and 250-percent decrease and 0- and 12-percent increase in the loss coefficient at respective inflow angles of 0°, 15.2°, and 20.6° when compared with results observed for no control at the respective inflow angles. The increase in pressure coefficient realized with this vortex-generator arrangement and other small-span arrangements results from improvement in the conversion of kinetic energy to static pressure by delaying or eliminating separation; consequently, little improvement should be expected for diffusers encountering no separation. Other arrangements were efficient at large inflow angles and inefficient at small ones.

One vortex-generator arrangement (arrangement 25) having generators on both walls was found to be reasonably insensitive to inflow angles as large as 20.6°. No separation, almost constant high-pressure coefficients, low-loss coefficients except for 0° inflow, and good whirl reduction were observed with this arrangement. An increase in the pressure coefficient of approximately 23 percent above that for the diffuser without generators to a value 75 percent of that possible for an ideal fluid was observed for an inflow angle of 20.6°.

It should be realized that the large-span generators tested are essentially inefficient stators. Improved performance can, no doubt, be accomplished by improving the stator design.

Radial distribution.- Distribution of exit static pressure, total pressure, and whirl angle for the three inflow angles for which tests were conducted are presented in figure 21. It appears (fig. 21) that, as the inflow angle increases, the total and static pressures near the outer wall increase, the total and static pressures near the inner wall

decrease, and the exit whirl angles increase. The effects of a particular vortex-generator arrangement on the distributions are similar for each inflow angle tested.

Longitudinal static pressure.- A plot of the longitudinal static pressures along both walls of the diffuser for the arrangements having generators on both walls is presented for the three inflow angles in figure 22. With this arrangement the inflow angle has little influence on changes of static pressure occurring along the diffuser walls.

CONCLUSIONS

The following conclusions are drawn as to the effect of vortex generators on the performance of an annular diffuser with a whirling inlet flow. The diffuser is of the annular straight-wall type having an outer diameter of 21 inches, an area ratio 1.9 to 1, and a fully developed pipe flow at the diffuser inlet. Results were obtained for three inlet whirl angles, 0°, 15.2°, and 20.6°. Rectangular noncambered airfoils which were used as vortex generators and as straightening vanes were varied in chord, span, angle setting, number, and location.

1. For the diffuser with no flow control, decreases in the static-pressure coefficient were noted with increases in inlet whirl angle. Values of static pressure coefficient of 0.52, 0.50, and 0.47, respectively, were obtained for the diffuser with inlet whirl angles of 0°, 15.2°, and 20.6°.

2. Separation from the diffuser inner wall was observed for mean inlet whirl angles of 0° and 15.2°. Separation was eliminated with small-span vortex generators. One arrangement $\left(24\right.$ 3-inch-chord, $\frac{1}{2}$-inch-span vortex generators set counterrotating at $\left.\pm 15^\circ\right)$ gave values of the static-pressure coefficient for the 0°, 15.2°, and 20.6° inlet whirl angles of 0.60, 0.56, and 0.48. This value of 0.60 was the maximum obtained in this investigation and occurred with 0° inlet whirl angle.

3. One large-span, multiple vortex-generator arrangement $\left(24\right.$ 3-inch-chord, $\frac{1}{2}$-inch-span vortex generators set counterrotating at $\pm 15^\circ$ and located on the inner wall and 24 3-inch-chord, $3\frac{1}{8}$-inch-span vortex generators set corotating at 0° and located on the outer wall$\left.\right)$ was found to be reasonably insensitive to whirl angles as high as 20.6°. No separation, almost constant high static-pressure recovery, low total pressure loss, and good whirl reduction were observed with this arrangement. An increase

in static-pressure rise of approximately 23 percent above that observed for no control was realized for the highest angle of whirl. This arrangement represented the best compromise for all inlet whirl angles tested.

4. For this diffuser with an inlet whirl angle of 20.6°, straightening of the flow and, consequently, conversion of the tangential kinetic energy was necessary to realize significant increases in the static-pressure coefficient; for inlet whirl angles of 15.2° or less, where separation was encountered near the diffuser inlet, a greater improvement in the static-pressure coefficient was realized by controlling separation than by straightening the flow.

Langley Aeronautical Laboratory,
National Advisory Committee for Aeronautics,
Langley Field, Va.

REFERENCES

1. Wood, Charles C.: Preliminary Investigation of the Effects of Rectangular Vortex Generators on the Performance of a Short 1.9:1 Straight-Wall Annular Diffuser. NACA RM L51G09, 1951.

2. Bohm, H., and Koppe, M.: The Influence of Friction on Steady Diffuser Flows at High Speeds. B.I.G.S.-47, Joint Intelligence Objectives Agency, Washington, D. C., July 23, 1946.

3. Schwartz, Ira R.: Investigations of an Annular Diffuser-Fan Combination Handling Rotating Flow. NACA RM L9B28, 1949.

TABLE I.- VORTEX-GENERATOR ARRANGEMENTS TESTED

Arrangement	Chord, in.	Span, in.	Set	Angle setting of adjacent airfoils, deg	Number of generators	Diffuser wall	Location upstream (+) or downstream (-) from cylinder-cone junction, in.	Inlet whirl angle		
								20.6°	15.2°	0°
1	3	1/2	Counterrotating	±15	24	Inner	1	x	x	x
2	3	1/2	------do-------	6, 36	24	-do--	1	x	x	x
3	3	1/2	------do-------	-5, 25	24	-do--	1	x	-----	--
4	2	1/2	------do-------	±15	24	-do--	1	x	x	x
	3	2	Corotating	0	16	-do--	-9			
5	3	1/2	------do-------	6	24	-do--	1	x	-----	--
6	3	1/2	------do-------	-2	24	-do--	1	x	-----	--
7	3	1/2	------do-------	-9	24	-do--	1	x	-----	--
8	3	1/2	------do-------	-15	24	-do--	1	x	x	x
9	3	1	------do-------	4	24	-do--	1	x	-----	--
10	3	1	------do-------	0	24	-do--	1	x	-----	--
11	3	1	------do-------	-4	24	-do--	1	x	-----	--
12	3	1	------do-------	-9	24	-do--	1	x	-----	--
13	3	$1\frac{9}{16}$	------do-------	0	24	-do--	1	x	x	--
14	3	$1\frac{9}{16}$	------do-------	-4	24	-do--	1	x	-----	--
15	3	$1\frac{9}{16}$	------do-------	-9	24	-do--	1	x	-----	--
16	3	$3\frac{1}{8}$	------do-------	2	24	-do--	1	x	x	--
17	3	$3\frac{1}{8}$	------do-------	0	24	-do--	1	x	x	--
18	3	$3\frac{1}{8}$	------do-------	-3	24	-do--	1	x	x	--
19	3	$1\frac{9}{16}$	------do-------	-4	12	-do--	1	x	-----	--
20	3	$1\frac{9}{16}$	------do-------	-4	48	-do--	1	x	-----	--
21	2	1	------do-------	-4	24	-do--	1	x	x	--
22	1	1	------do-------	-4	24	-do--	1	x	x	--
23	3	$3\frac{1}{8}$	------do-------	0	24	-do--	1			
	3	1/2	Counterrotating	±15	24	-do--	$-3\frac{1}{2}$	x	-----	--
24	3	$3\frac{1}{8}$	Corotating	0	24	Outer	2	x	x	--
25	3	$3\frac{1}{8}$	Corotating	0	24	Outer	2	x	x	x
	3	1/2	Counterrotating	±15	24	Inner	1			

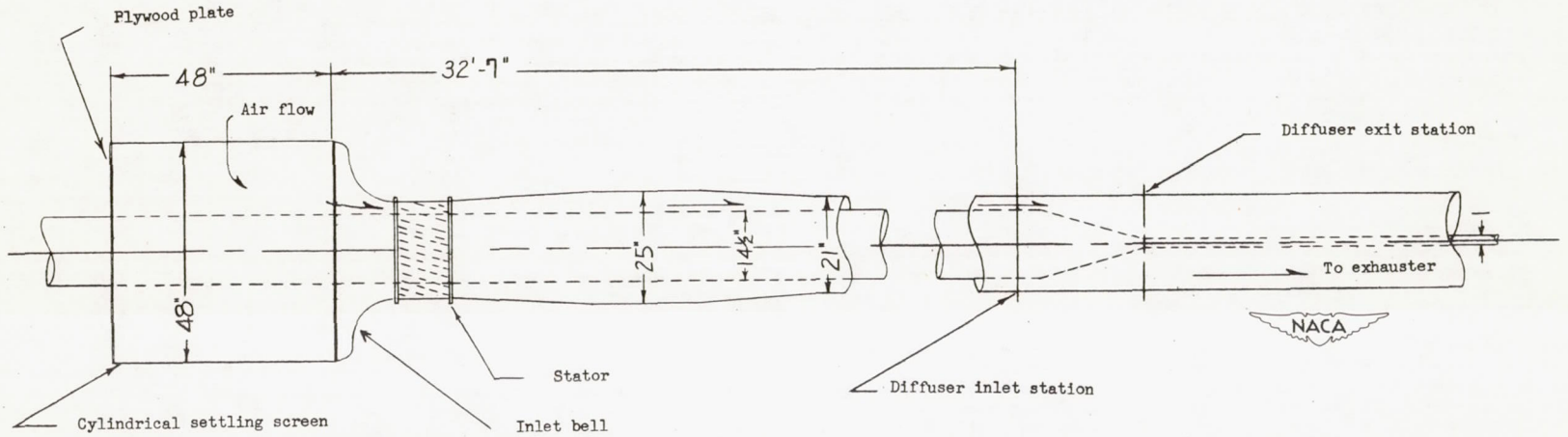

Figure 1.- Schematic diagram of experimental setup.

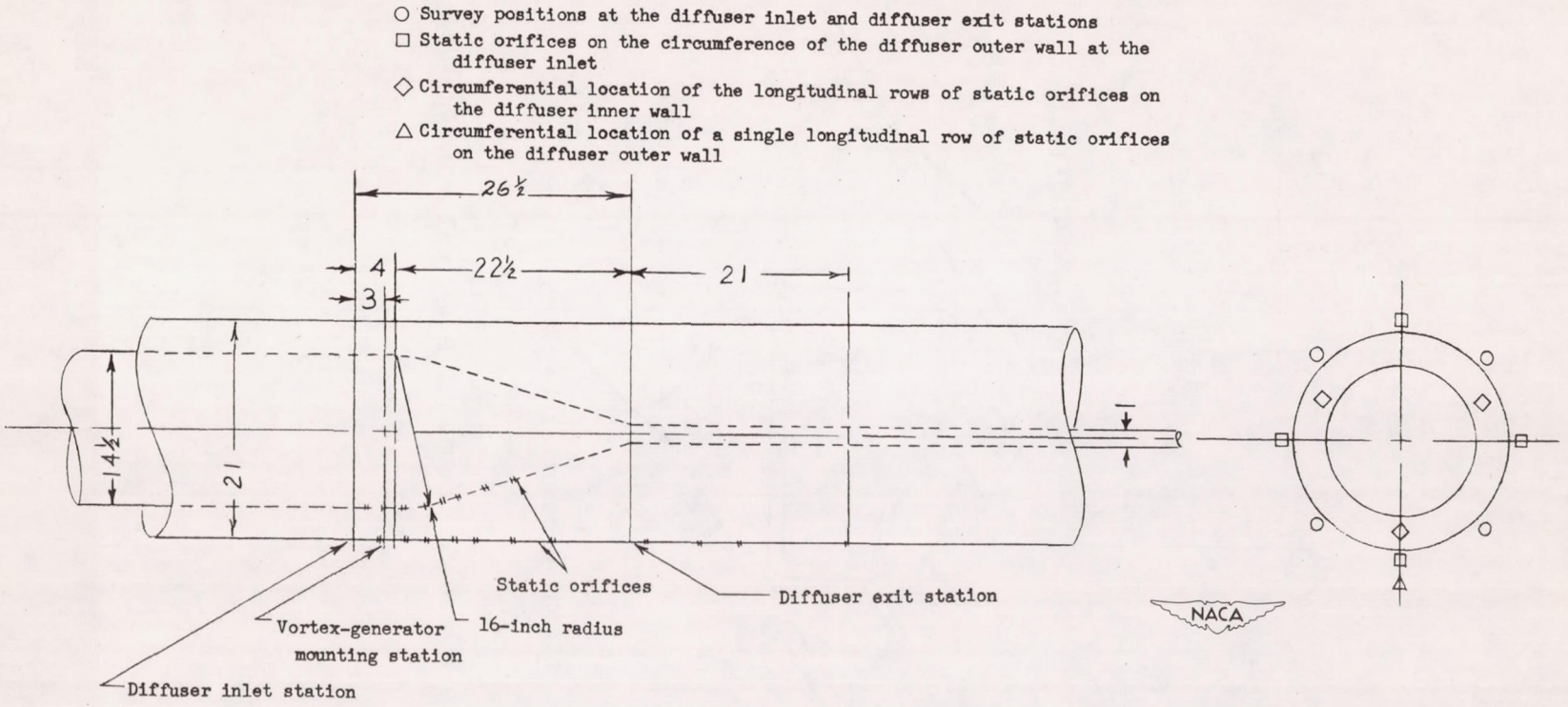

Figure 2.- Schematic diagram of the diffuser tested. All dimensions are in inches.

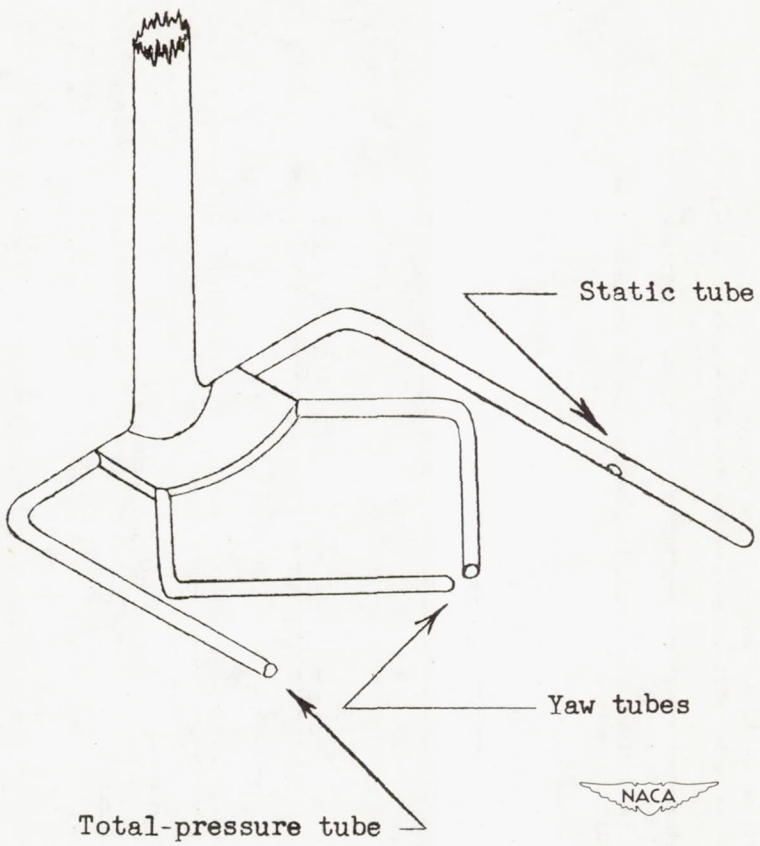

Figure 3.- Schematic diagram of a typical survey instrument.

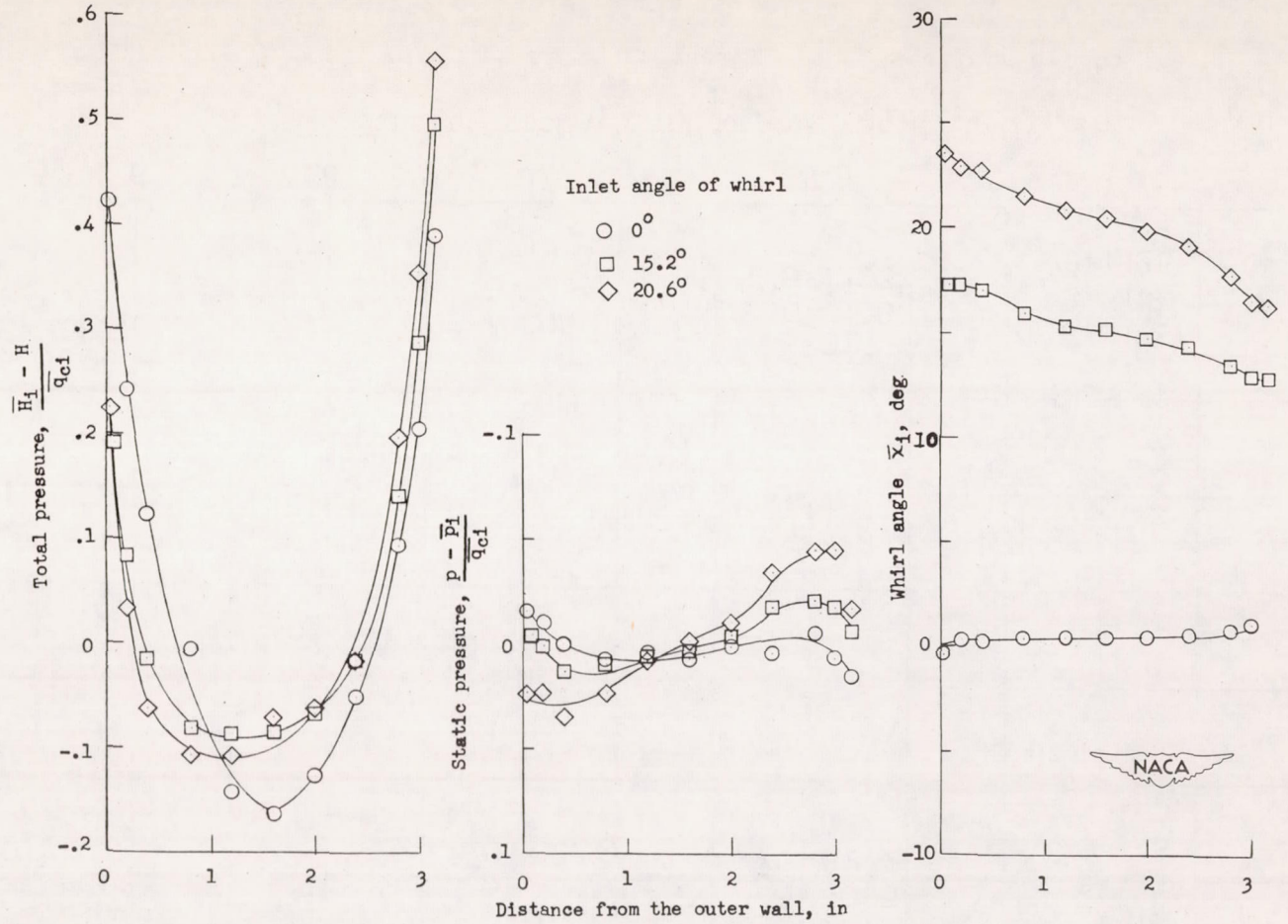

Figure 4.- Radial variations of total pressure, static pressure, and whirl angle at the diffuser inlet for various inlet whirl angles. $\frac{\overline{p}_i}{\overline{H}_{ia}} \approx 0.95$.

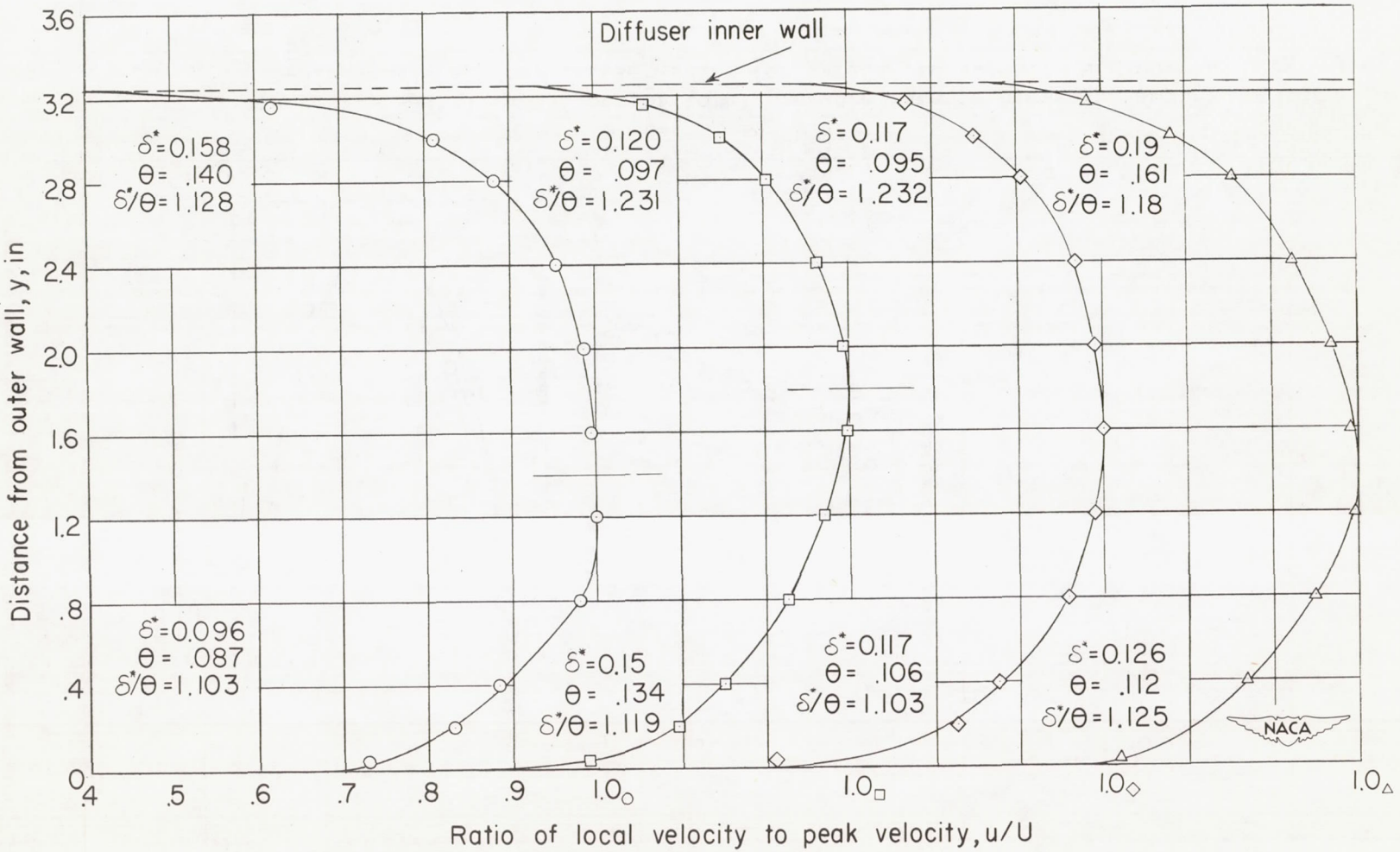

Figure 5.- Velocity profiles at four equally spaced sections around the diffuser inlet station. Inlet angle of whirl, $\bar{x}_i = 0^\circ$; $\frac{\bar{p}_i}{\bar{H}_{ia}} \approx 0.95$.

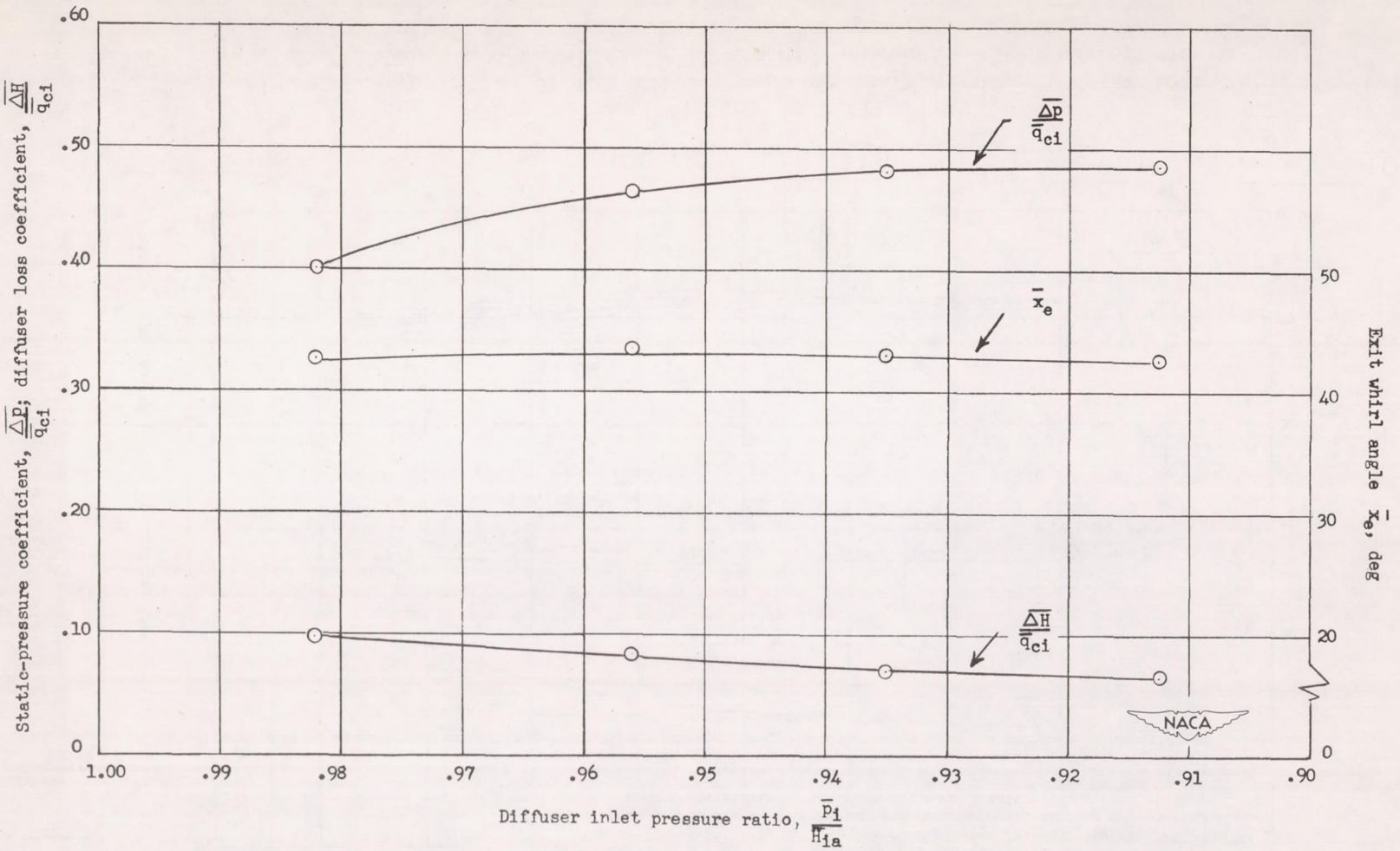

Figure 6.- Variation of the static-pressure coefficient, diffuser loss coefficient, and whirl angle at the diffuser exit with inlet pressure ratio for the diffuser with no control. $\overline{x}_i = 20.6^\circ$.

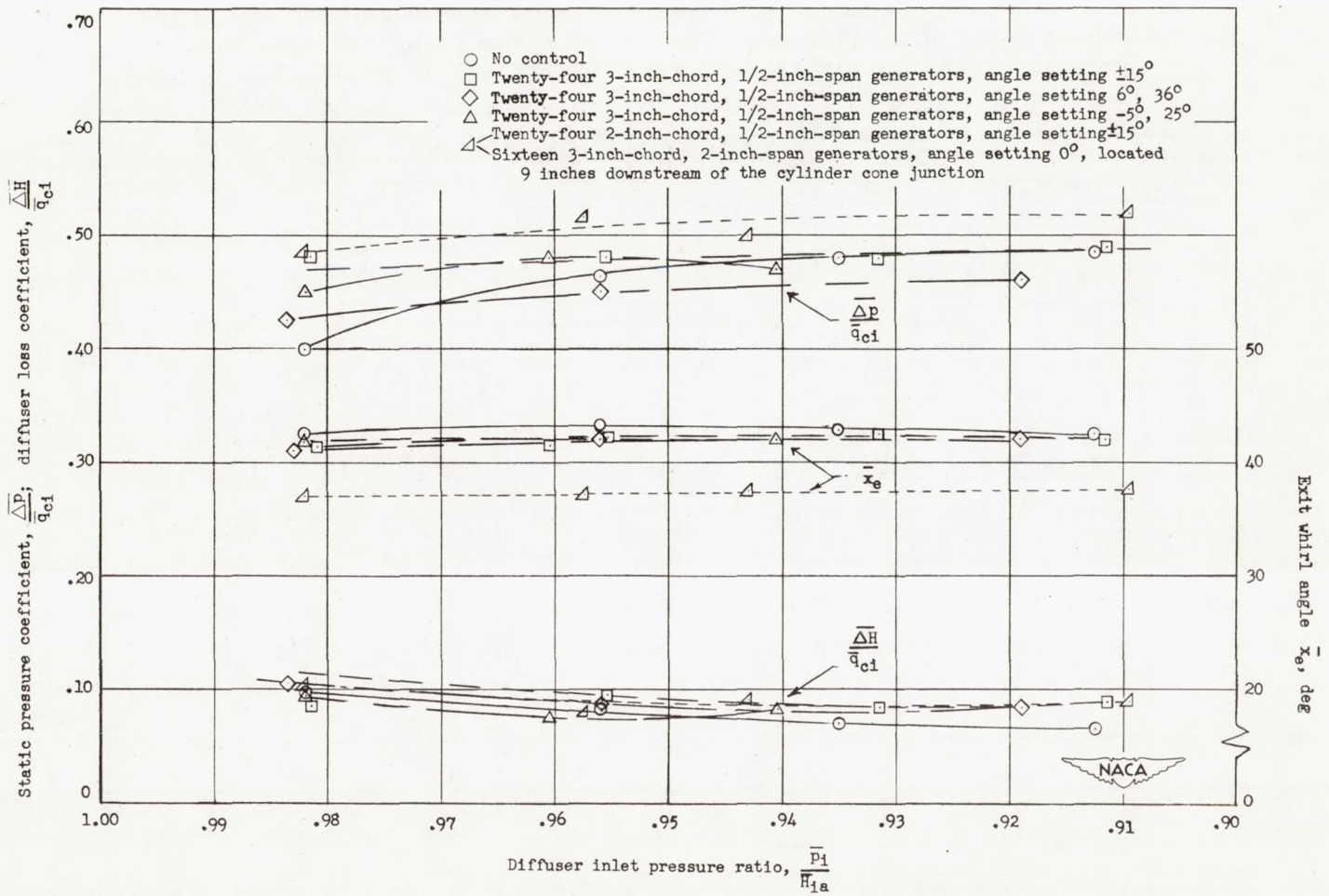

Figure 7.- Variation of the static-pressure coefficient, diffuser loss coefficient, and whirl angle at the diffuser exit with inlet pressure ratio for various counterrotating vortex-generator arrangements. $\bar{x}_i = 20.6^\circ$.

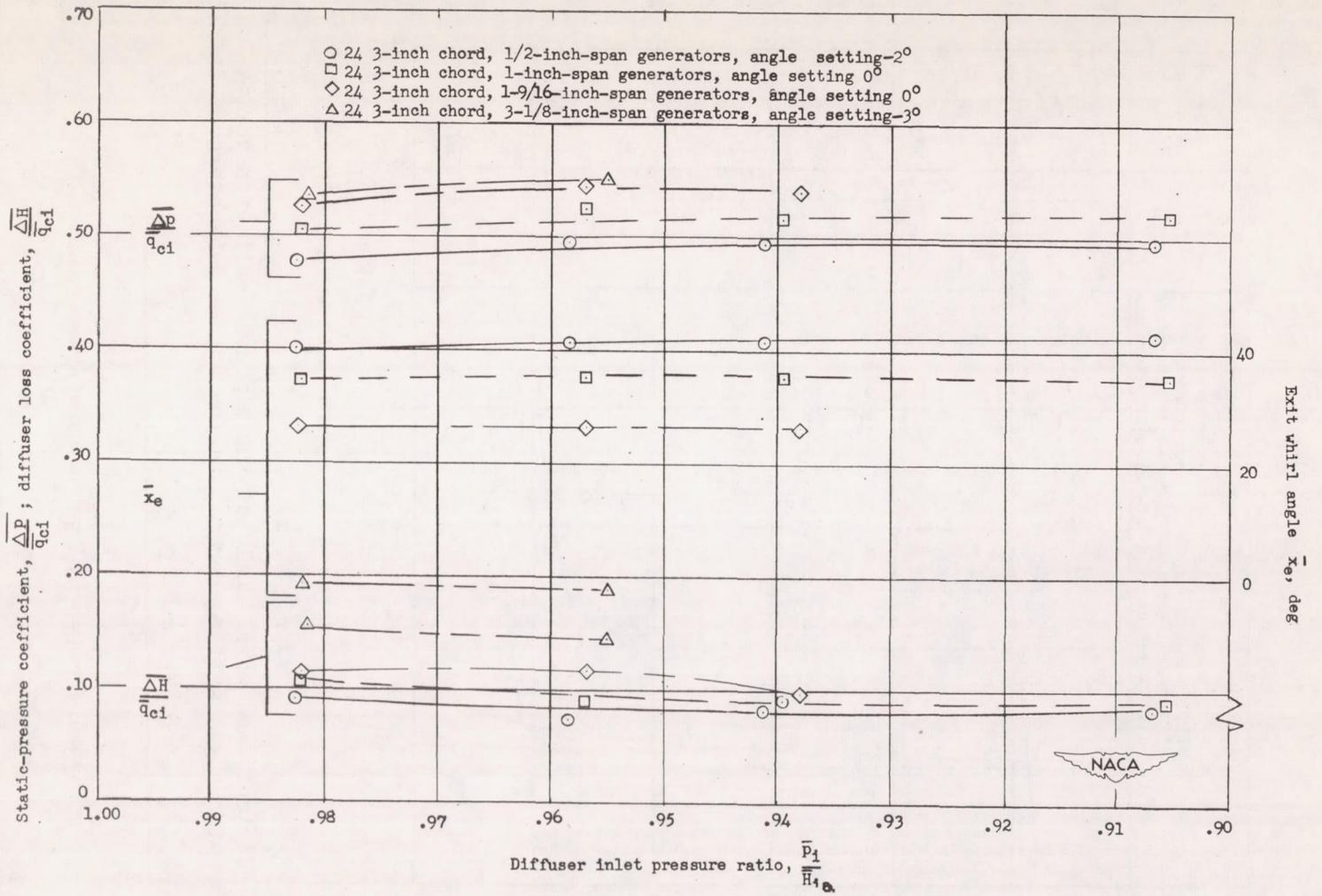

Figure 8.- Variation of the static-pressure coefficient, diffuser loss coefficient, and whirl angle at the diffuser exit with inlet pressure ratio for corotating vortex generators of different spans.

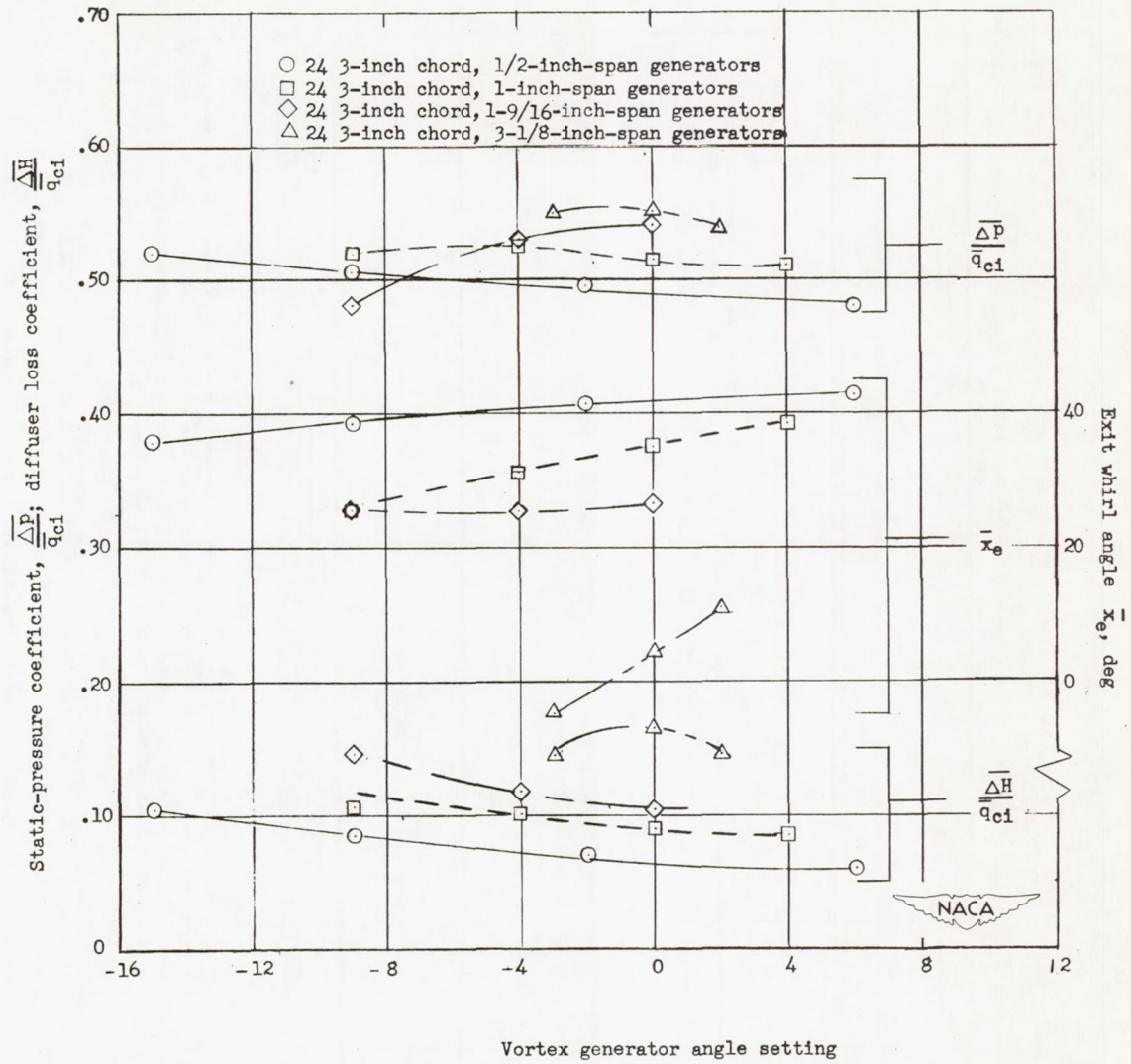

Figure 9.- Variation of the static-pressure coefficient, diffuser loss coefficient, and whirl angle at the diffuser exit with vortex-generator angle setting for corotating vortex-generators of different spans. $\bar{x}_i = 20.6^\circ$; $\frac{\overline{p}_i}{\overline{H}_{ia}} = 0.95$.

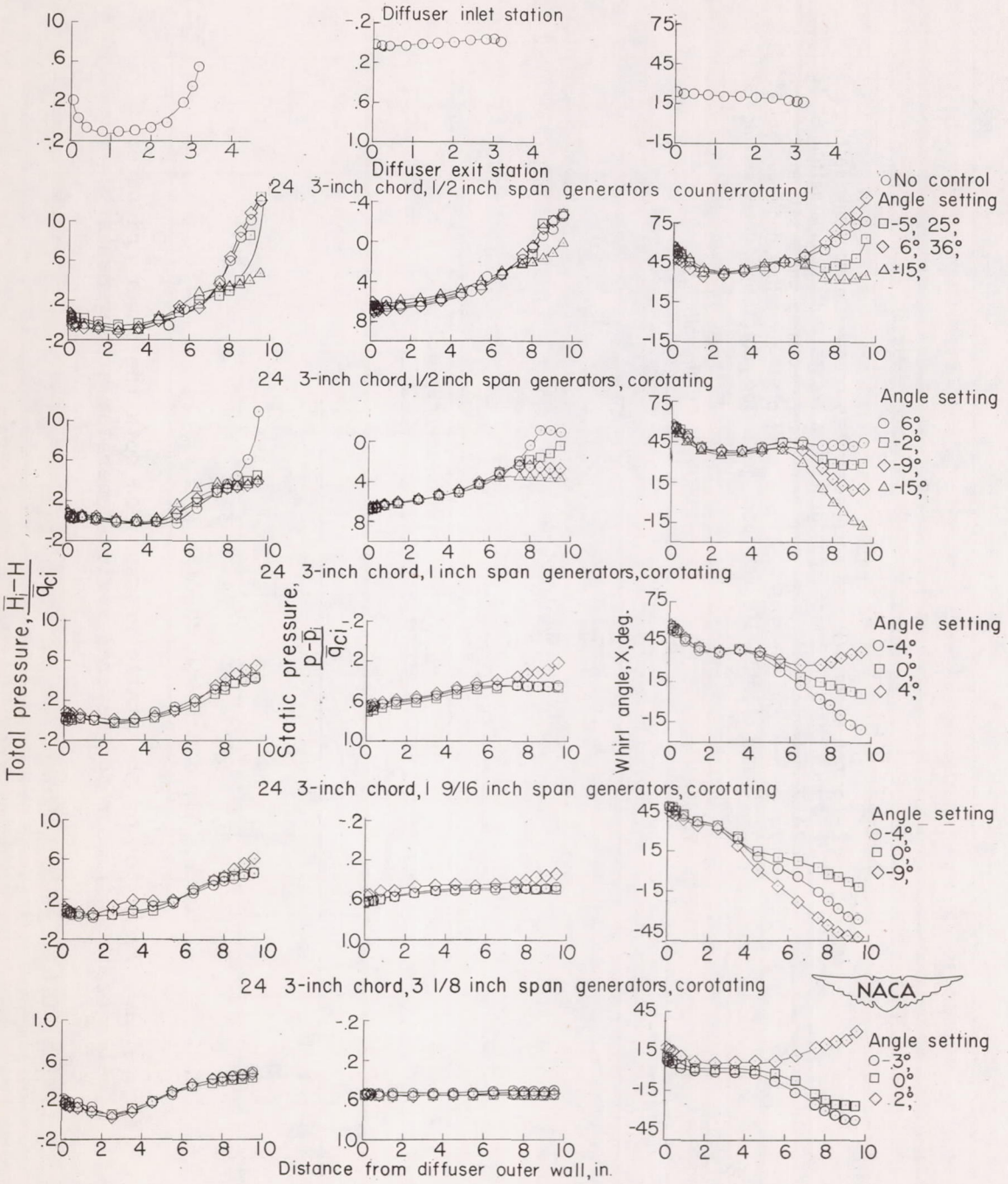

Figure 10.- Radial variation of total pressure, static pressure, and whirl angle at the diffuser exit station for vortex generators with different spans and angle settings. $\bar{x}_i = 20.6^\circ$; $\frac{\bar{p}_i}{\bar{H}_{ia}} \approx 0.95$.

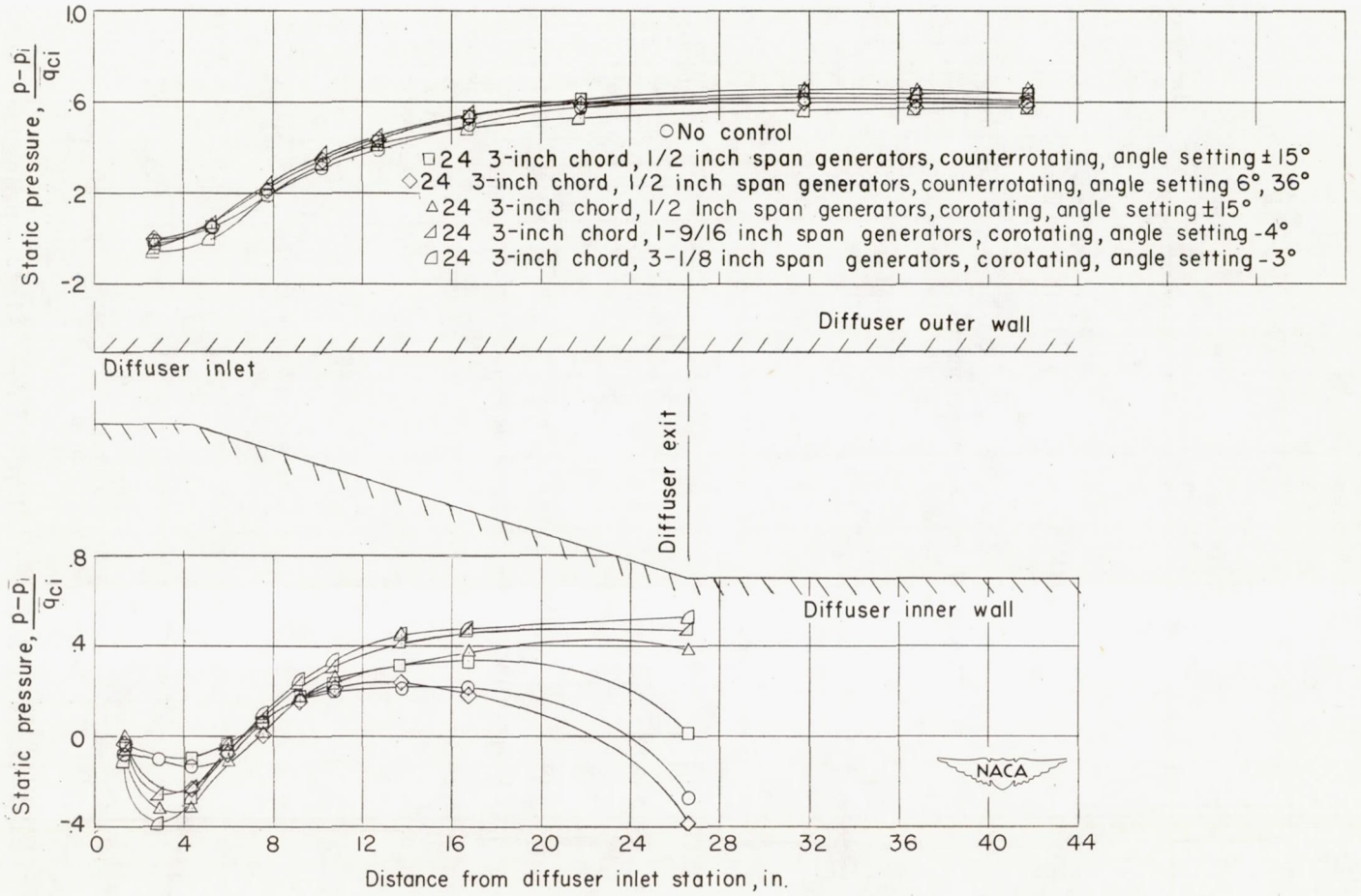

Figure 11.- Variation of the static pressure on both the inner and outer walls of the diffuser for several vortex-generator arrangements.

$\bar{x}_i = 20.6°$; $\frac{\bar{p}_i}{\bar{H}_{ia}} \approx 0.95$.

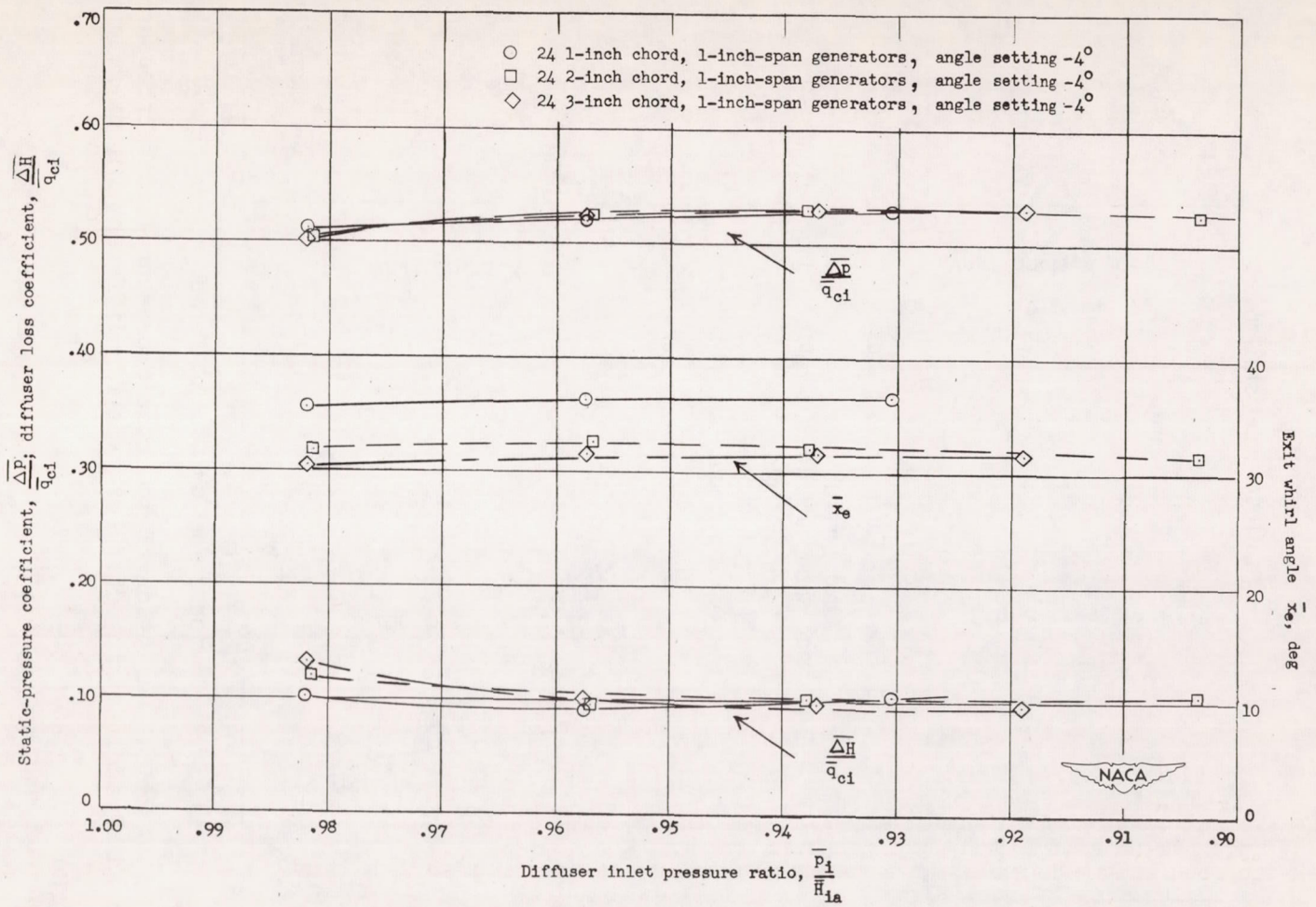

Figure 12.- Variation of the static-pressure coefficient, diffuser loss coefficient, and whirl angle at the diffuser exit with inlet pressure ratio for corotating vortex generators of different chords. $\bar{x}_i = 20.6°$.

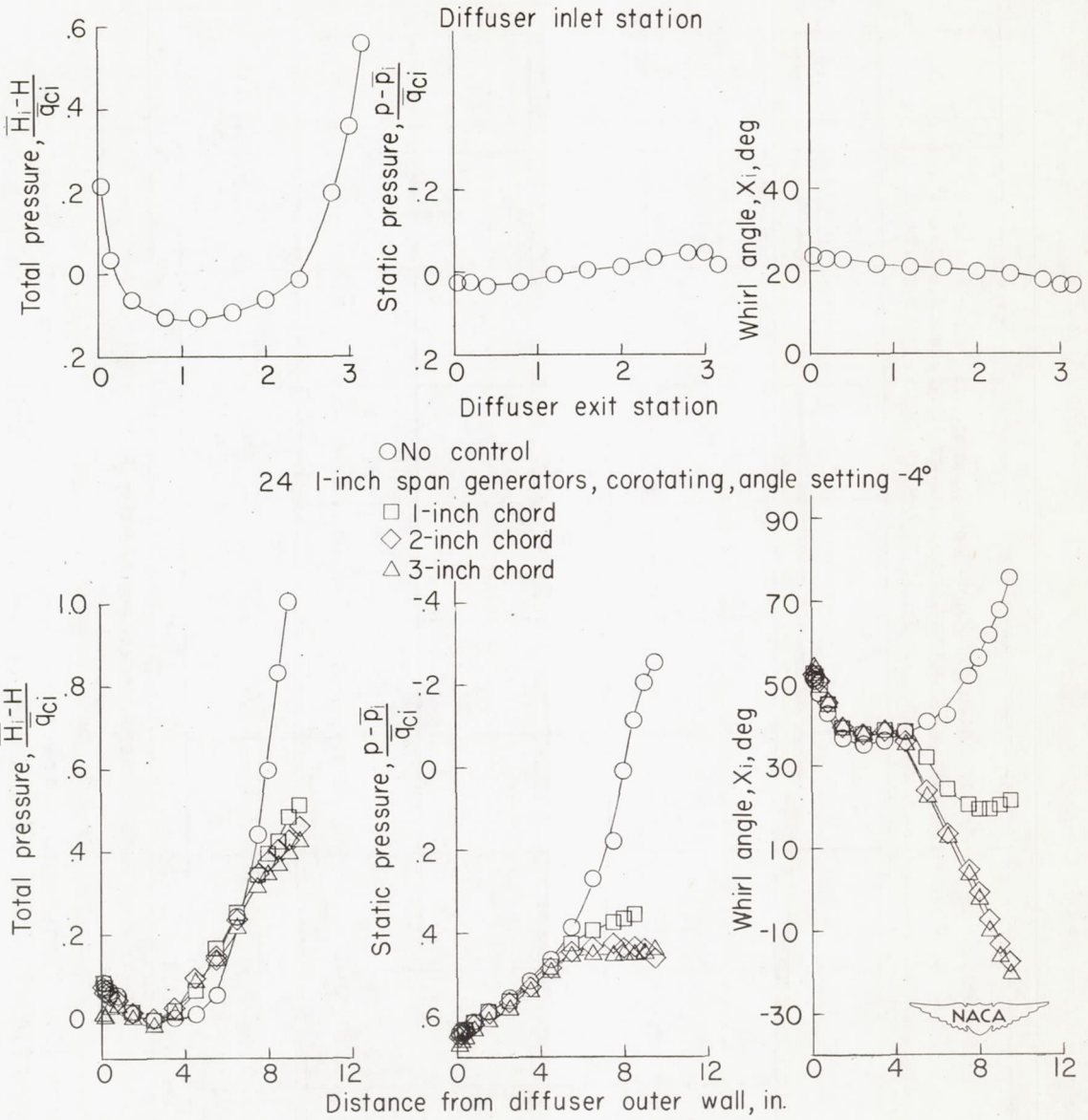

Figure 13.- Radial variation of the static pressure, total pressure, and whirl angle at the diffuser exit for different vortex-generator chords. $\bar{x}_i = 20.6°$; $\frac{\bar{p}_i}{\bar{H}_{ia}} \approx 0.95$.

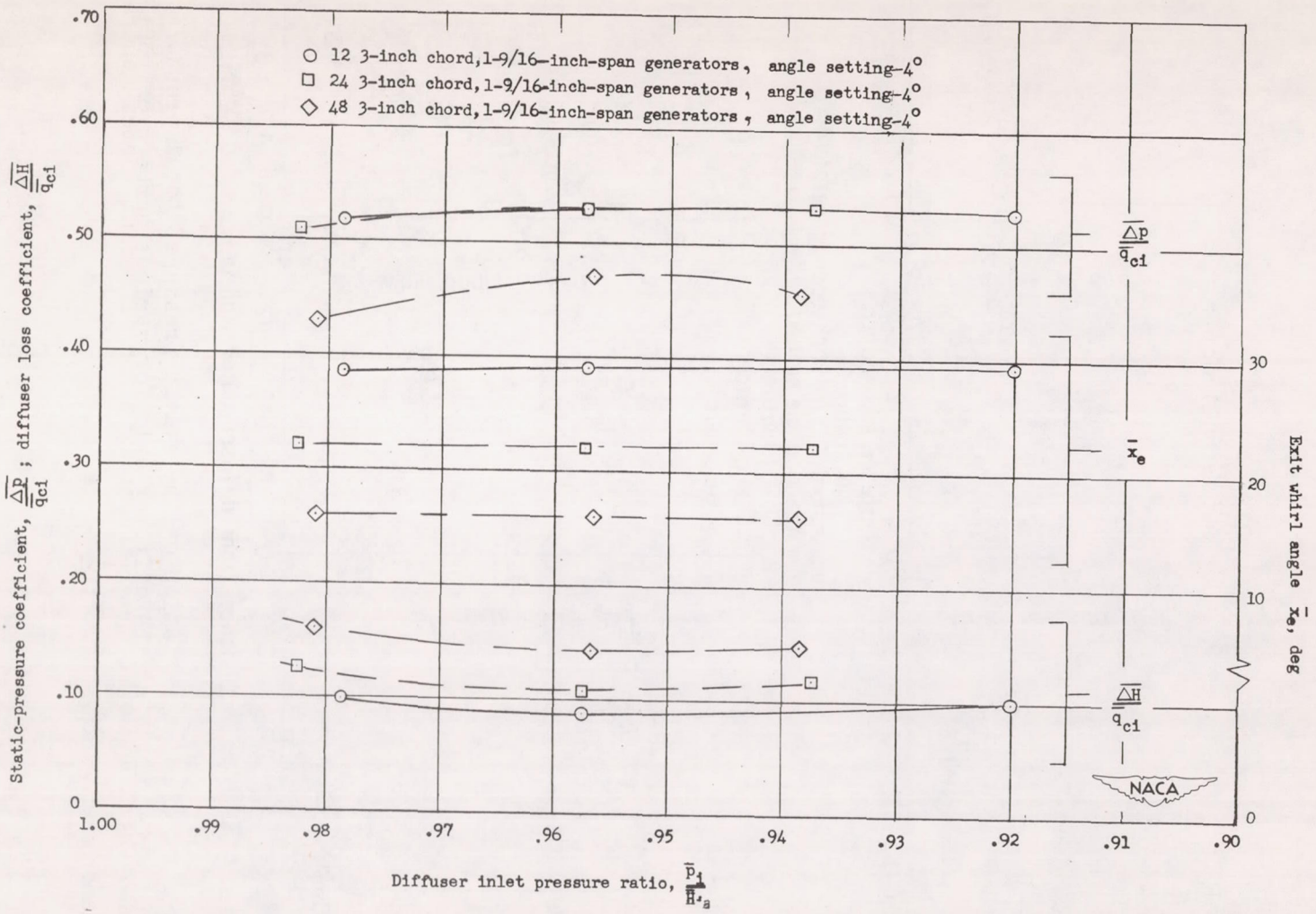

Figure 14.- Variation of the static-pressure coefficient, diffuser loss coefficient, and whirl angle at the diffuser exit with inlet pressure ratio for various numbers of vortex generators. $\overline{x}_i = 20.6^\circ$.

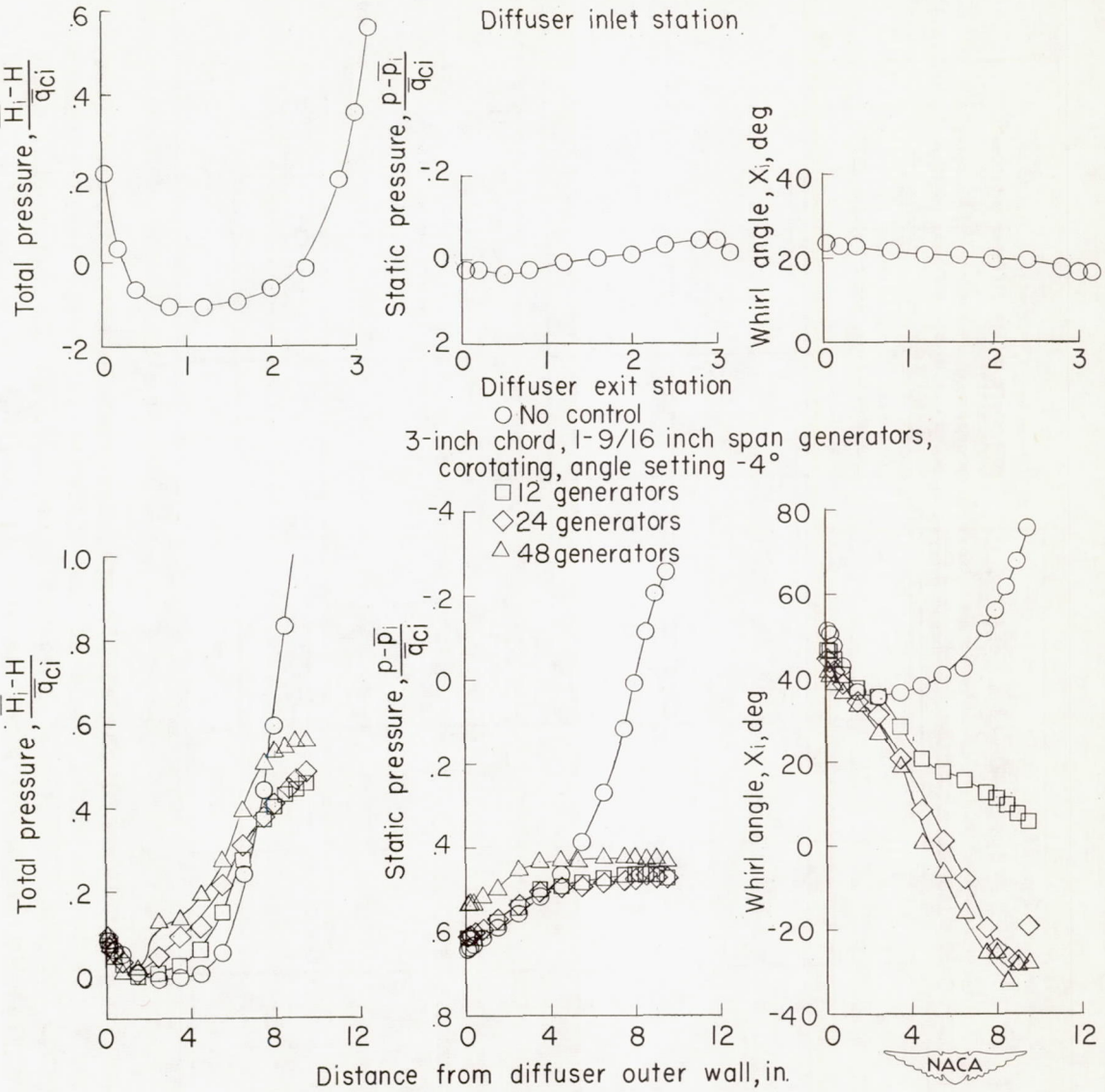

Figure 15.- Radial variation of the static pressure, total pressure, and whirl angle at the diffuser exit for various numbers of vortex generators. $\bar{x}_i = 20.6°$; $\frac{\bar{p}_i}{\bar{H}_{ia}} \approx 0.95$.

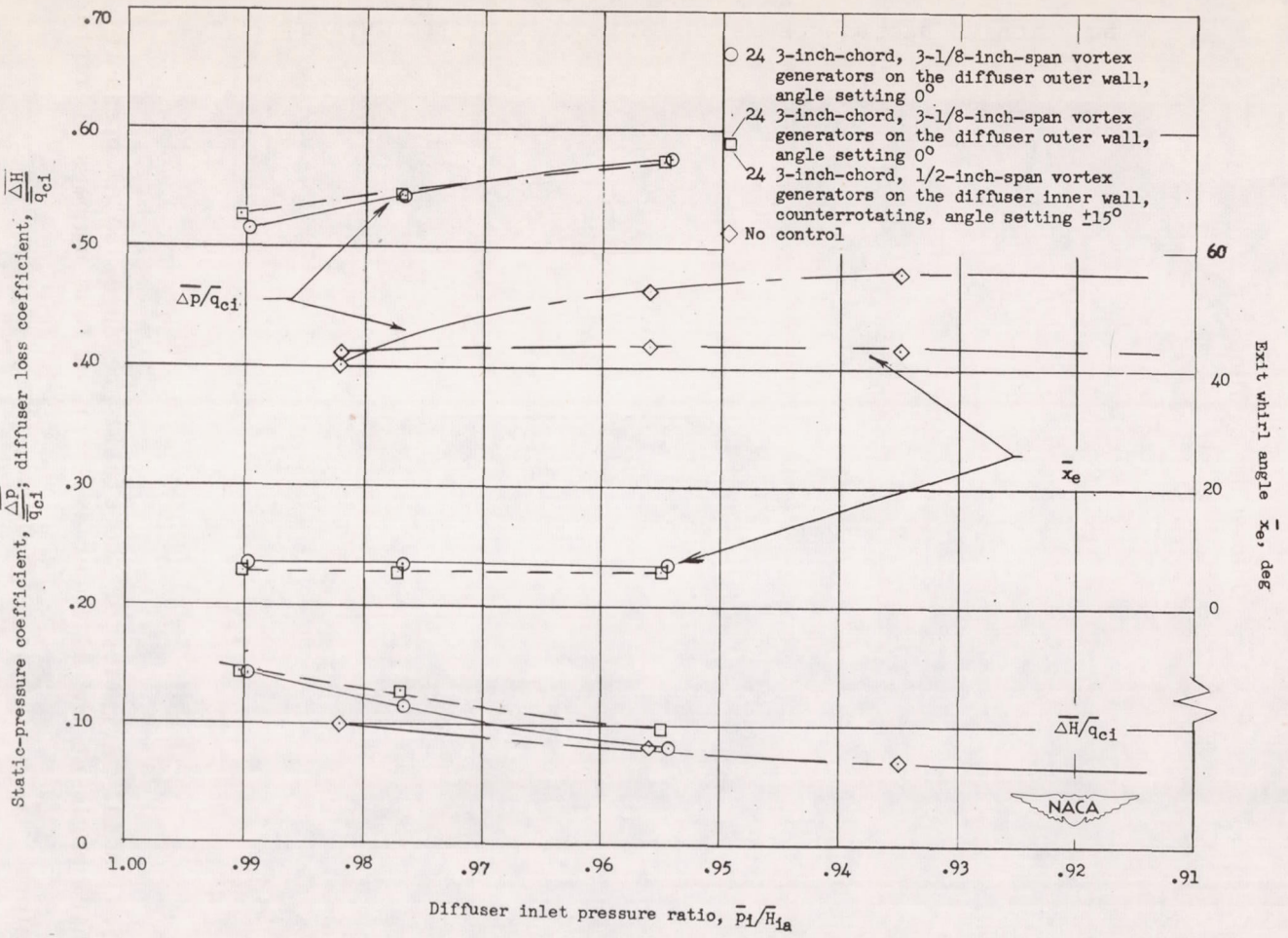

Figure 16.- Variation of the static-pressure coefficient, diffuser loss coefficient, and whirl angle at the diffuser exit with inlet pressure ratio for the diffuser with vortex generators on the outer wall and on both the inner and outer walls. $\overline{x}_i = 20.6^\circ$.

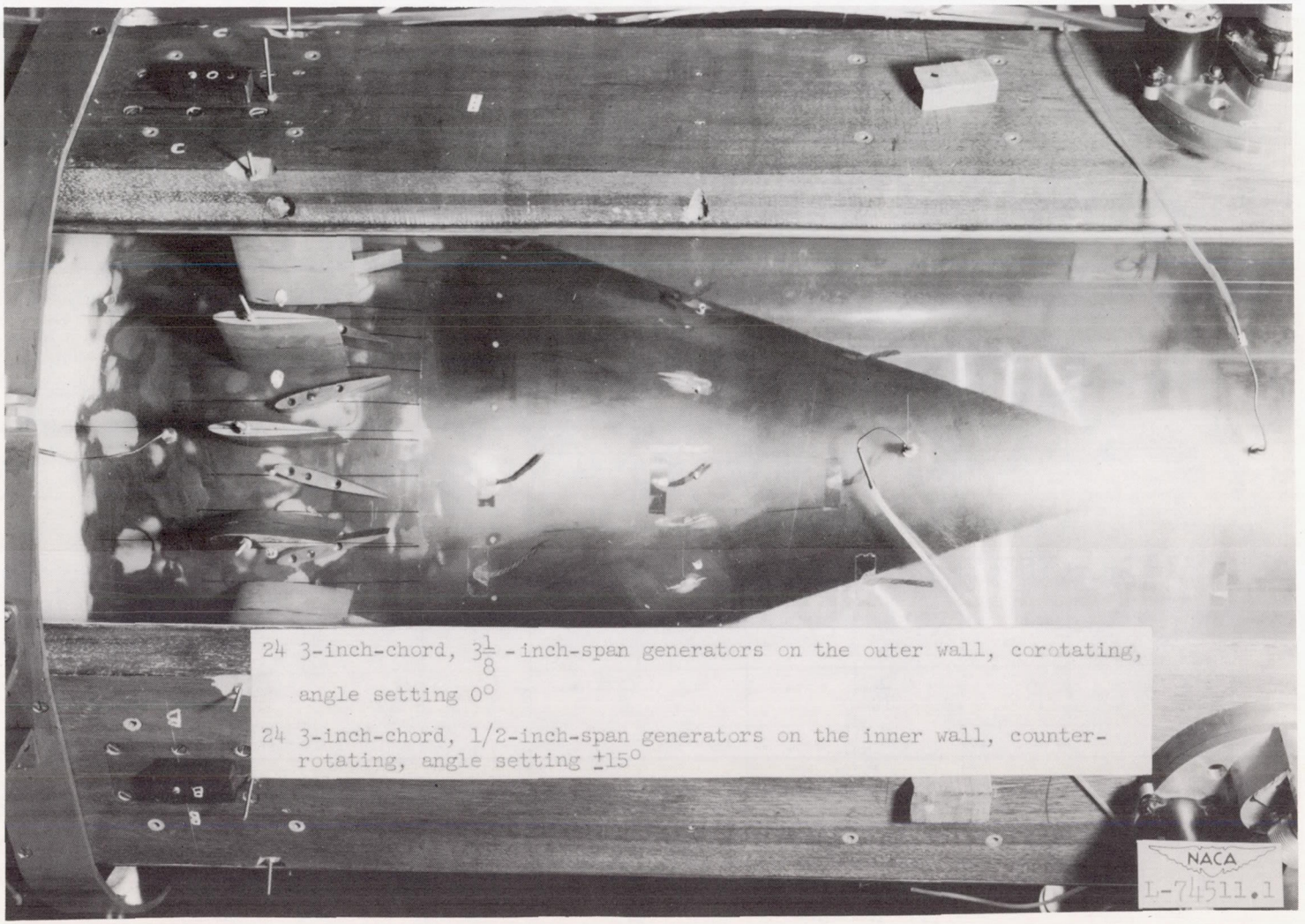

Figure 17.- Annular diffuser showing vortex generators on both the diffuser inner and outer walls.

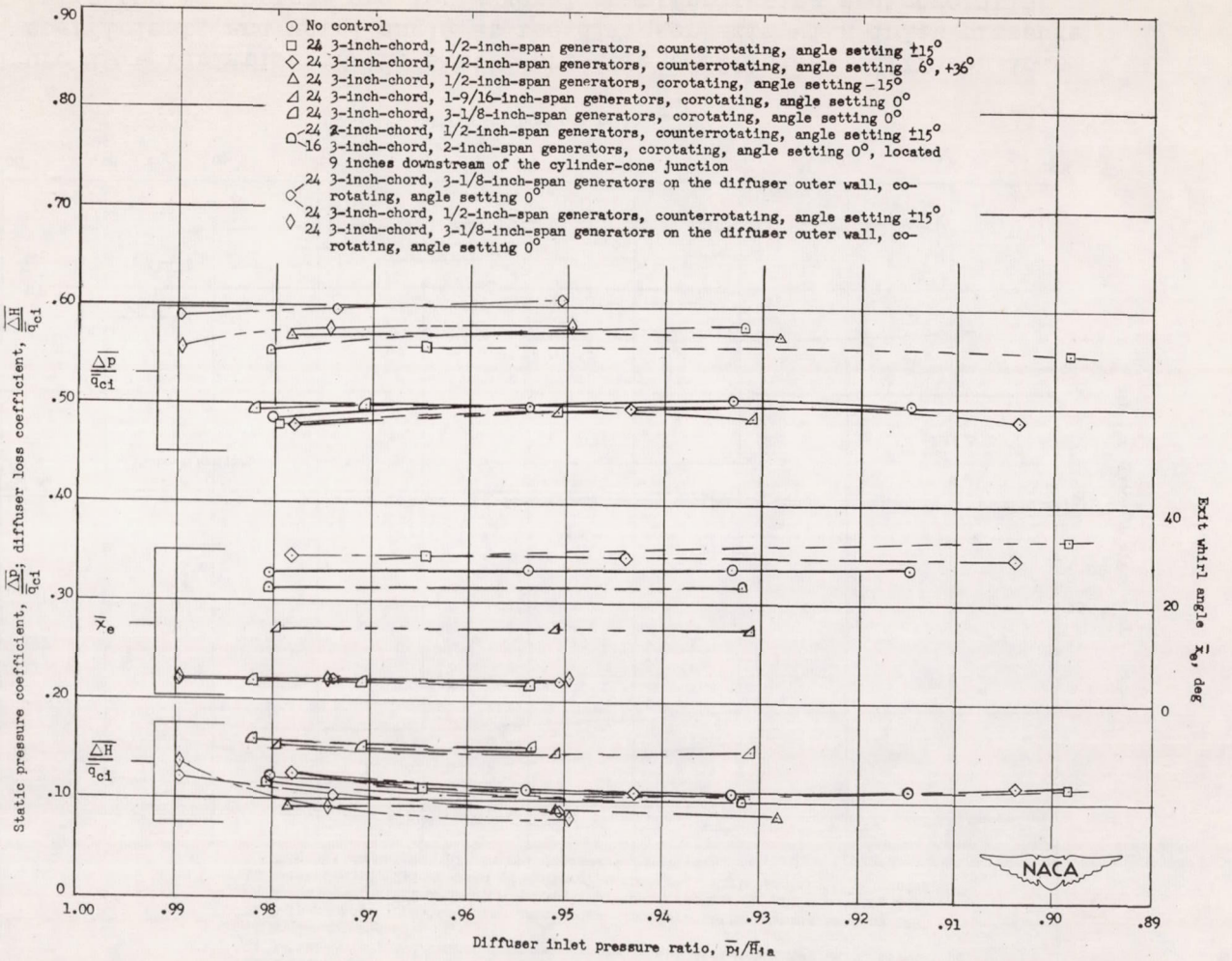

Figure 18.- Variation of the static-pressure coefficient, diffuser loss coefficient, and whirl angle at the diffuser exit with inlet pressure ratio for no control and for several counterrotating and corotating vortex-generator arrangements. $\overline{x}_i = 15.2^\circ$.

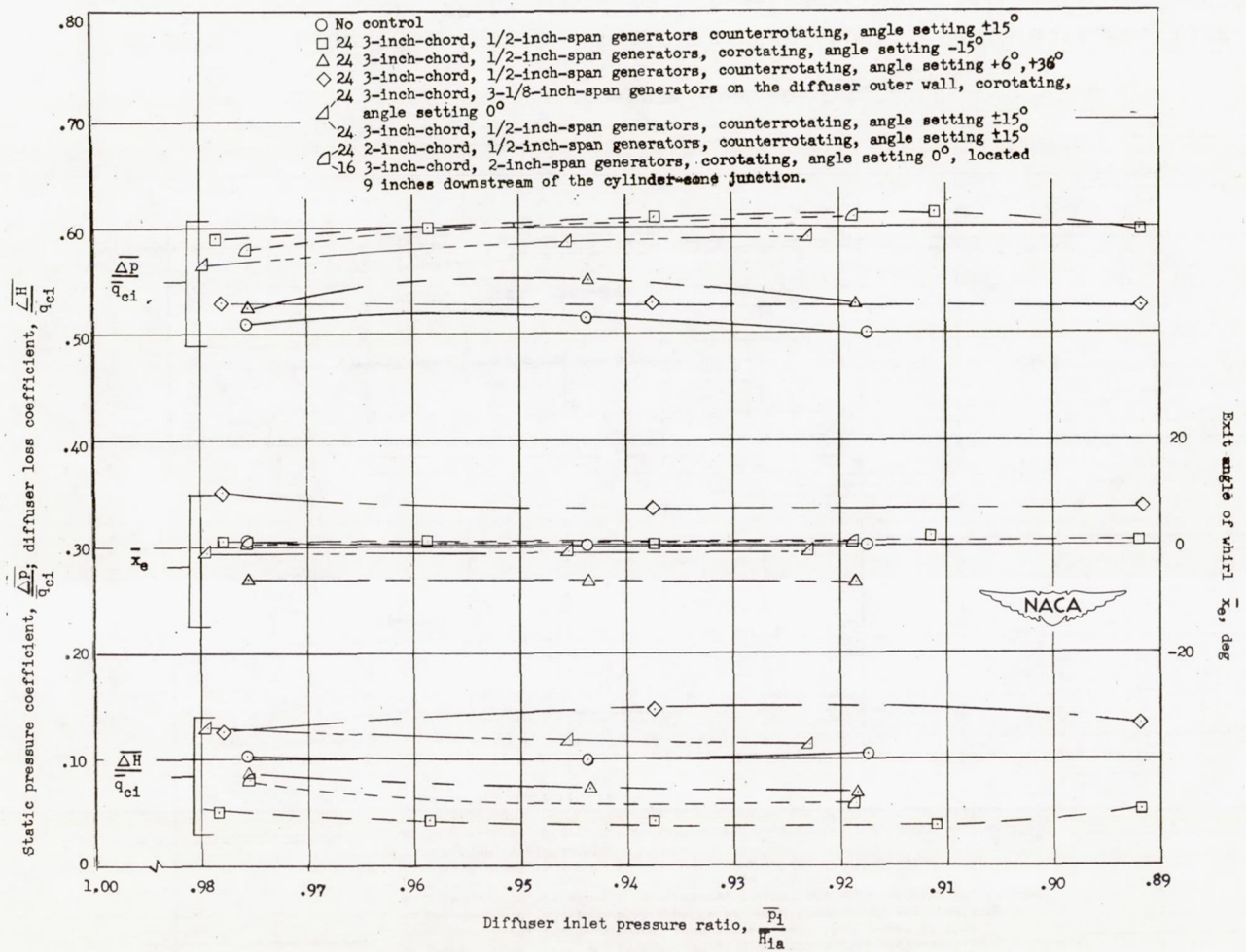

Figure 19.- Variation of the static-pressure coefficient, diffuser loss coefficient, and whirl angle at the diffuser exit with inlet pressure ratio for no control and for several counterrotating and corotating vortex-generator arrangements. $\bar{x}_i = 0^\circ$.

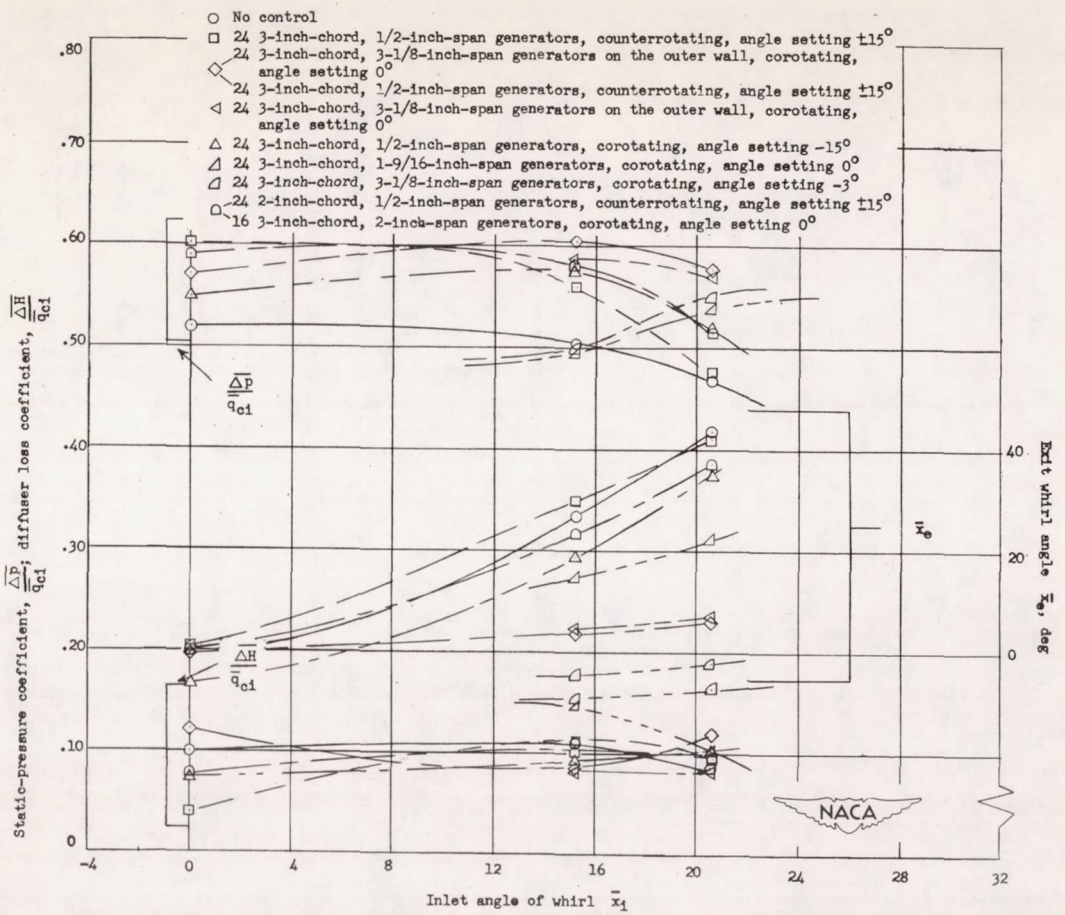

Figure 20.- Variation of the static-pressure coefficient, diffuser loss coefficient, and whirl angle at the diffuser exit with inlet angle of whirl for no control and for several counterrotating and corotating vortex-generator arrangements. $\frac{\bar{p}_1}{\bar{H}_{1a}} = 0.95$.

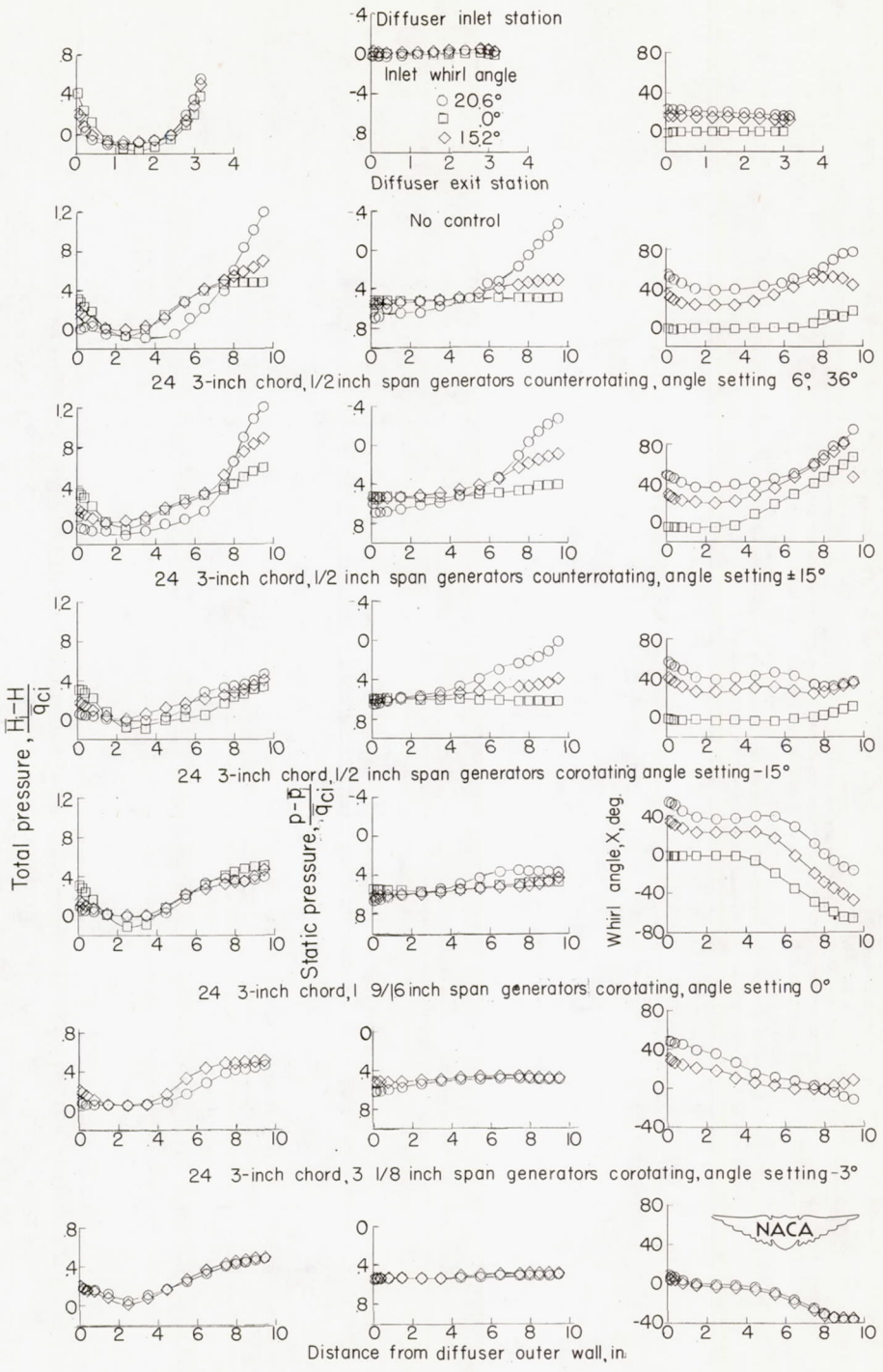

(a) Vortex generators on the diffuser inner wall.

Figure 21.- Radial variation of the total pressure, static pressure, and whirl angle for several vortex-generator arrangements at the various whirl angles tested. $\frac{\bar{p}_i}{\bar{H}_{ia}} \approx 0.95$.

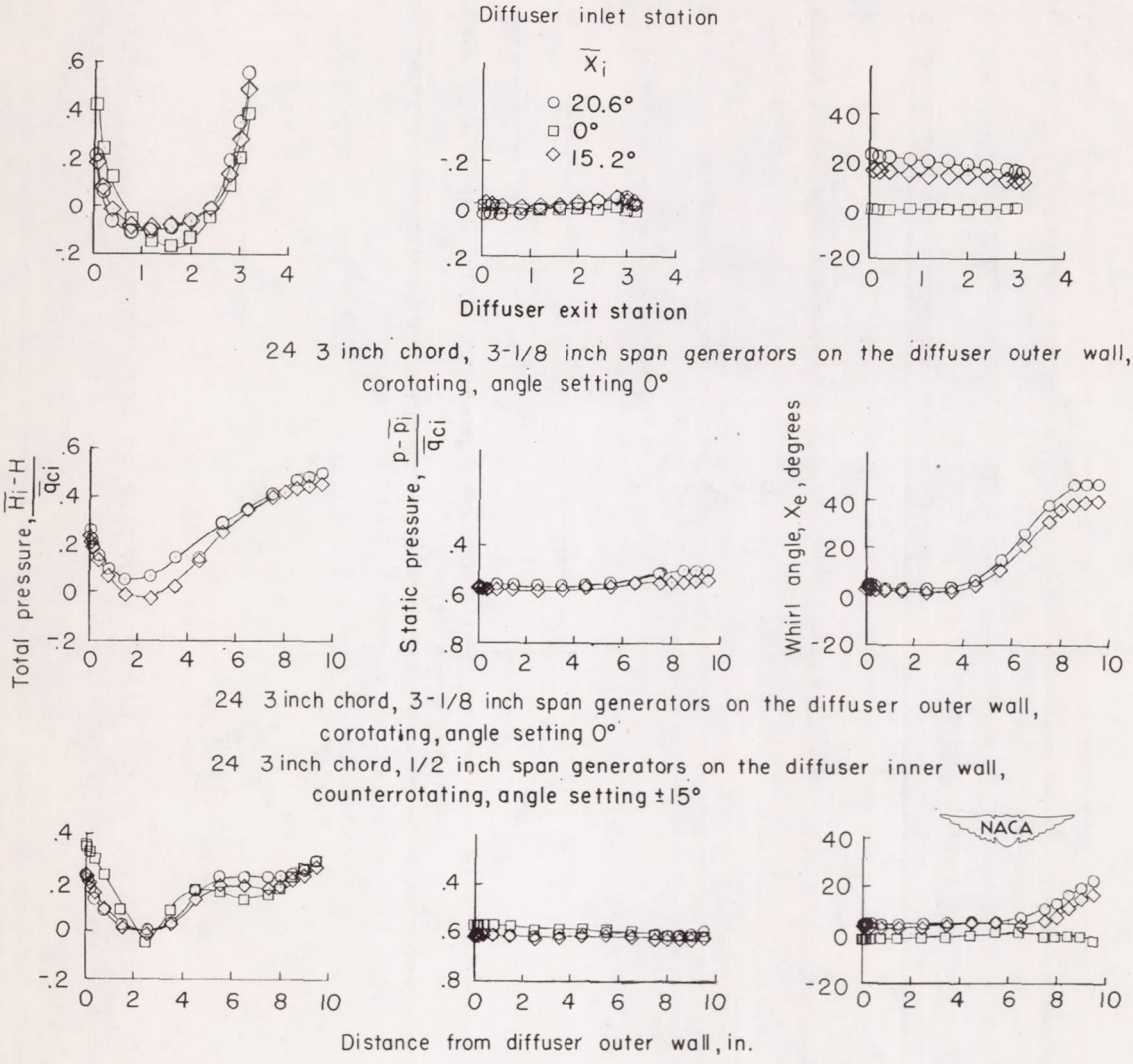

(b) Vortex generators on the diffuser outer wall and on both the diffuser outer and inner walls.

Figure 21.- Concluded.

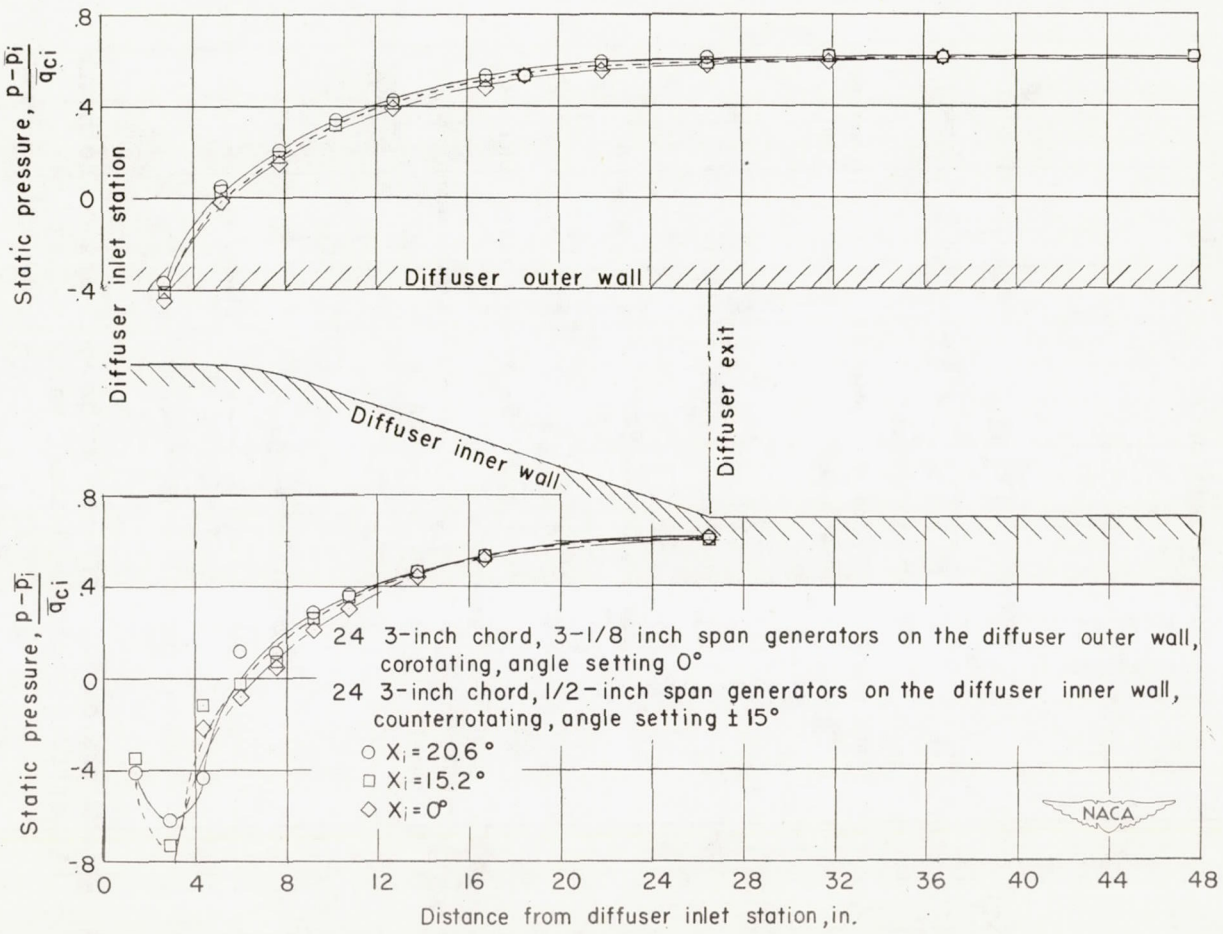

Figure 22.- Variation of the static pressure on the inner and outer walls of the diffuser at various inlet angles of whirl. $\bar{x}_i$ for the diffuser having vortex generators on both walls. $\frac{\bar{p}_i}{\bar{H}_{ia}} \approx 0.95$.